Neural Network Adaptive Output Feedback Control for Intensive Care Unit Sedation and Intraoperative Anesthesia

Wassim M. Haddad, *Senior Member, IEEE*, James M. Bailey, Tomohisa Hayakawa, *Member, IEEE*, and Naira Hovakimyan, *Senior Member, IEEE*

***Abstract*—The potential applications of neural adaptive control for pharmacology, in general, and anesthesia and critical care unit medicine, in particular, are clearly apparent. Specifically, monitoring and controlling the depth of anesthesia in surgery is of particular importance. Nonnegative and compartmental models provide a broad framework for biological and physiological systems, including clinical pharmacology, and are well suited for developing models for closed-loop control of drug administration. In this paper, we develop a neural adaptive output feedback control framework for nonlinear uncertain nonnegative and compartmental systems with nonnegative control inputs. The proposed framework is Lyapunov-based and guarantees ultimate boundedness of the error signals. In addition, the neural adaptive controller guarantees that the physical system states remain in the nonnegative orthant of the state space. Finally, the proposed approach is used to control the infusion of the anesthetic drug propofol for maintaining a desired constant level of depth of anesthesia for noncardiac surgery.**

***Index Terms*—Adaptive control, automated anesthesia, bispectral index (BIS), dynamic output feedback, electroencephalography, neural networks, nonlinear nonnegative systems, nonnegative control, set-point regulation.**

I. Introduction

CONTROL engineering has impacted almost every aspect of modern life, with applications ranging from relatively simple systems, such as thermostats and automotive cruise control, to highly complex systems, such as advanced tactical fighter aircraft and variable-cycle gas turbine aeroengines. Control technology has also had an impact on modern medicine in areas such as robotic surgery, electrophysiological systems (pacemakers and automatic implantable defibrillators), life support (ventilators, artificial hearts), and image-guided therapy and surgery. However, there remain barriers to the application of modern control theory and technology to medicine. These barriers include system uncertainties, inherent to biology, that limit mathematical modeling and the ability to apply many of the tools of modern control technology. An additional impediment is the relatively limited communication between control engineers and the medical community. One area of medicine most suited for applications of control technology is clinical pharmacology in which mathematical modeling has had a predominant role [1], [2]. This discipline includes *pharmacokinetics*, the relationship between drug dose and the resultant tissue concentrations as a function of time, and *pharmacodynamics*, the relationship between tissue concentration and drug effect. The mathematical foundation for pharmacokinetic and pharmacodynamic modeling is nonnegative and compartmental dynamical systems theory [2]–[7] and so it is easy to see why control theory and technology may have much to offer clinical pharmacology.

Nonnegative and compartmental models provide a broad framework for biological and physiological systems, including clinical pharmacology, and are well suited for the problem of closed-loop control of drug administration. Specifically, nonnegative and compartmental dynamical systems [2]–[7] are composed of homogeneous interconnected subsystems (or compartments) which exchange variable nonnegative quantities of material with conservation laws describing transfer, accumulation, and elimination between the compartments and the environment. It thus follows from physical considerations that the state trajectory of such systems remains in the nonnegative orthant of the state space for nonnegative initial conditions [7]. Thus, it is not surprising that nonnegative and compartmental models have wide applicability in biology and medicine, and their use in the specific field of clinical pharmacology is particularly noteworthy [8].

It has long been appreciated that if one can identify a physiological variable that quantifies therapeutic drug effect and measures it continuously in real time, it should be possible to utilize feedback (closed-loop) control, implemented with a computer, to maintain this variable, and hence the drug effect, at the desired value. By their very nature, cardiovascular and central nervous functions are critical in the acute care environment, such as the operating room or the intensive care unit (ICU), and hence, mature technologies have evolved for their quantitative assessment. For this reason, the primary application of closed-loop control of drug administration has been to hemodynamic management

Manuscript received December 1, 2005; revised September 20, 2006; accepted February 5, 2007. This work was supported in part by the National Science Foundation under Grant ECS-0601311 and by the U.S. Air Force Office of Scientific Research under Grants FA9550-06-1-0240 and F49620-03-1-0443.

W. M. Haddad is with the School of Aerospace Engineering, Georgia Institute of Technology, Atlanta, GA 30332-0150 USA (e-mail: wm.haddad@aerospace.gatech.edu).

J. M. Bailey is with the Department of Anesthesiology, Northeast Georgia Medical Center, Gainsville, GA 30503 USA (e-mail: james.bailey@nghs.com).

T. Hayakawa is with the Department of Mechanical and Environmental Informatics, Tokyo Institute of Technology, Tokyo 332-0012, Japan (e-mail: hayakawa@mei.titech.ac.jp).

N. Hovakimyan is with the Department of Aerospace and Ocean Engineering, Virginia Polytechnic Institute and State University, Blacksburg, VA 24061 USA (e-mail: nhovakim@vt.edu).

Digital Object Identifier 10.1109/TNN.2007.899164

and, more recently, to control of levels of consciousness. As an example of the former application, the technology for the continuous measurement of blood pressure has been available for some time and systems have been developed to maintain blood pressure at the desired value in the operating room and ICU [9], [10].

The primary interest of our research has been in closed-loop control of the level of consciousness. While there is direct application of this research to the clinical task of operating room anesthesia, an application with potentially more impact is closed-loop control of level of consciousness of patients in ICUs. Mechanical ventilation is uncomfortable and causes anxiety in the patient. Appropriate sedation of mechanically ventilated ICU patients is very challenging. The common clinical scenario is a patient who is either undersedated and "fighting the ventilator" or is oversedated, with concomitant sequelae such as hypotension or prolonged emergence from sedation when it is deemed appropriate to begin weaning the patient from the ventilator. We can envision a future in which infusion pumps contain a small computer chip that allow the ICU nurse to connect the patient to the monitor of level of consciousness, feed the signal into the chip, which then drives the pump to titrate intravenous hypnotic drugs to the appropriate level of sedation. Given the shortage of experienced ICU nurses, we believe this would be a significant advance, allowing clinicians to focus on tasks other than titrating sedation.

In contrast to the control of hemodynamic variables, progress in the closed-loop control of anesthesia or sedation has been more difficult to attain. This has been primarily due to the lack of a method for measuring the depth of anesthesia. Ever since the pioneering work of Bickford [11], it has been known that the electroencephalograph (EEG) changes with the induction of anesthesia. However, the EEG is a complex of multiple time series and it is difficult to identify one component of the EEG which correlates with the clinical signs of anesthesia. Schwilden and his colleagues developed and clinically tested a closed-loop controller for the delivery of intravenous anesthesia using the median frequency of the EEG power spectrum as a performance variable [12]. Their system did not appear to offer any advantage over standard manual dosing control. It was unclear whether this was due to the algorithm or the deficiencies of the median EEG frequency as a measure of a depth of anesthesia. Subsequent to this early research, there has been substantial progress in the development of processed EEG monitors that analyze the raw data to extract a single measure of the depth of anesthesia. The best known of these monitors is the bispectral index (BIS) monitor.

The BIS is a single composite EEG measure that is well correlated with the depth of anesthesia [13], [14]. The BIS signal ranges from 0 (no cerebral electrical activity) to 100 (the normal awake state). All available evidence indicates that a BIS signal less than 60 is associated with lack of consciousness. With the commercial availability of a more reliable measure of consciousness, Absalom *et al.* developed a proportional–integral–derivative (PID) controller for the delivery of the intravenous agent propofol using the BIS signal as a performance variable [15]. This system exhibited undesirable oscillations inappropriate for clinical use. The most likely cause was the need for adaptive control. There is substantial variability among patients in the drug concentration at the locus of effect (the effect site) that results from a given dose (pharmacokinetic variability) and there is also substantial variability in the effect of a given concentration (pharmacodynamic variability). Furthermore, there may be pharmacokinetic and pharmacodynamic variability in the same patient at different points in time. PID controllers may be overly simplistic in the face of this variability. More recently, Struys and his colleagues have described an adaptive controller of the delivery of propofol anesthesia [16]. Clinical testing demonstrated acceptable performance, although as pointed out by Glass and Rampil [17], this may have been because the system was not highly stressed. In [16], a relatively high dose of the opioid remifentanil, a neurotransmitter inhibitor resulting in significant analgesic effect, was administered in conjunction to propofol. Consequently, central nervous system excitation due to surgical stimulus was blunted and, thus, the need to adjust the propofol dose as surgical stimulus was diminished. It is unknown whether the control system would have been effective in the absence of deep narcotization.

The algorithms of Schwilden *et al.* [12] and Struys *et al.* [16] were based on specific pharmacokinetic and pharmacodynamic models with fixed pharmacokinetic or pharmacodynamic parameters, respectively. However, there is a great deal of uncertainty about model selection and pharmacokinetic and pharmacodynamic parameter selection; models which are appropriate for one patient may not be appropriate for another patient. Model-independent control algorithms may be more useful. Given the complexity, uncertainties, and nonlinearities inherent in pharmacokinetic and pharmacodynamic models needed to capture the wide effects of pharmacological agents and anesthetics in the human body, neural networks can provide an ideal framework for developing adaptive controllers for clinical pharmacology. Neural networks consist of a weighted interconnection of fundamental elements called *neurons*, which are functions consisting of a summing junction and a nonlinear operation involving an activation function [18]. One of the primary reasons for the large interest in neural networks is their ability to approximate a large class of continuous nonlinear maps from the collective action of simple, autonomous processing units interconnected in simple ways. In addition, neural networks have attracted attention due to their inherently parallel and highly redundant processing architecture that makes it possible to develop parallel weight update laws. This parallelism makes it possible to effectively update a neural network online. These properties make neural networks a viable paradigm for adaptive system identification and control in clinical pharmacology.

In this paper, we extend the results of [19] and [20] to nonnegative and compartmental dynamical systems with applications to the specific problem of automated anesthesia. Specifically, we develop an output feedback neural network adaptive controller that operates over a tapped delay line (TDL) of available input and output measurements. The neuroadaptive laws for the neural network weights are constructed using a linear observer for the nominal normal form system error dynamics. The approach is applicable to a general class of nonlinear nonnegative dynamical systems without imposing a strict positive real requirement

on the transfer function of the linear error normal form dynamics [21]. Furthermore, since in pharmacological applications involving active drug administration control inputs as well as the system states need to be nonnegative, the proposed neuroadaptive output feedback controller also guarantees that the control signal as well as the physiological system states remain nonnegative. We emphasize that the proposed framework addresses adaptive *output feedback* controllers for nonlinear nonnegative and compartmental systems with *unmodeled dynamics* of *unknown dimension* while guaranteeing ultimate boundedness of the error signals corresponding to the physical system states as well as the neural network weighting gains. Output feedback controllers are crucial in clinical pharmacology since key physiological (state) variables cannot be measured in practice or in real time.

The contents of the paper are as follows. In Section II, we provide mathematical preliminaries on nonlinear nonnegative dynamical systems that are necessary for developing the main results of this paper. In Section III, we develop Lyapunov-like theorems for partial boundedness and partial ultimate boundedness for nonlinear dynamical systems necessary for obtaining less conservative ultimate bounds for neuroadaptive controllers as compared to ultimate bounds derived using classical boundedness and ultimate boundedness notions. In Section IV, we present our main neuroadaptive output feedback control framework for adaptive set-point regulation of nonlinear uncertain nonnegative and compartmental dynamical systems. In Section V, we develop a new and novel nonlinear pharmacokinetic and pharmacodynamic model for the intravenous anesthetic drug propofol. To demonstrate the efficacy of the proposed neuroadaptive control framework, we apply our framework to control the infusion of propofol for maintaining a desired constant level of depth of anesthesia for noncardiac surgery. In Section VI, we validate our neuroadaptive feedback control algorithm for clinical pharmacology via a series of clinical evaluation trials. The clinical trials demonstrate excellent regulation of unconsciousness allowing for a safe and effective administration of the anesthetic agent propofol. Finally, in Section VII, we draw some conclusions.

II. Mathematical Preliminaries

In this section, we introduce notation, several definitions, and some key results concerning nonlinear nonnegative dynamical systems [7], [22]–[24] that are necessary for developing the main results of this paper. Specifically, for $x \in \mathbb{R}^n$, we write $x \geq\geq 0$ (respectively, $x \gg 0$) to indicate that every component of x is nonnegative (respectively, positive). In this case, we say that x is *nonnegative* or *positive*, respectively. Likewise, $A \in \mathbb{R}^{n\times m}$ is *nonnegative*[1] or *positive* if every entry of A is nonnegative or positive, respectively, which is written as $A \geq\geq 0$ or $A \gg 0$, respectively. Let $\overline{\mathbb{R}}_+^n$ and $\mathbb{R}_+^n$ denote the nonnegative and positive orthants of $\mathbb{R}^n$, that is, if $x \in \mathbb{R}^n$, then $x \in \overline{\mathbb{R}}_+^n$ and $x \in \mathbb{R}_+^n$ are equivalent, respectively, to $x \geq\geq 0$ and $x \gg 0$. Furthermore, we write $(\cdot)^{\mathrm{T}}$ to denote transpose, $\mathrm{tr}(\cdot)$ for the trace operator, $\lambda_{\min}(\cdot)$ to denote the minimum eigenvalue of a Hermitian matrix, $\|\cdot\|$ for a vector norm, $\|\cdot\|_{\mathrm{F}}$ for the Frobenius matrix norm, and $V'(x)$ for the Fréchet derivative of V at x. Finally, $M \otimes N$ denotes the Kronecker product of matrices M and N. The following definition introduces the notion of a nonnegative (respectively, positive) function.

Definition 2.1: Let $T > 0$. A real function $u : [0, T] \to \mathbb{R}^m$ is a *nonnegative* (respectively, *positive*) *function* if $u(t) \geq\geq 0$ (respectively, $u(t) \gg 0$) on the interval $[0, T]$.

Definition 2.2 introduces the notion of essentially nonnegative vector fields [7], [25].

Definition 2.2: Let $f = [f_1, \cdots, f_n]^{\mathrm{T}} : \mathcal{D} \to \mathbb{R}^n$, where $\mathcal{D}$ is an open subset of $\mathbb{R}^n$ that contains $\overline{\mathbb{R}}_+^n$. Then, f is *essentially nonnegative* if $f_i(x) \geq 0$, for all $i = 1, \ldots, n$, and $x \in \overline{\mathbb{R}}_+^n$ such that $x_i = 0$, where x_i denotes the ith element of x.

Note that if $f(x) = Ax$, where $A \in \mathbb{R}^{n\times n}$, then f is essentially nonnegative if and only if A is essentially nonnegative, that is, $A_{(i,j)} \geq 0$, $i, j = 1, \ldots, n, i \neq j$, where $A_{(i,j)}$ denotes the (i, j)th entry of A.

In this paper, we consider controlled nonlinear dynamical systems of the form

$$\dot{x}(t) = f(x(t)) + G(x(t))u(t) \quad x(0) = x_0, \qquad t \geq 0 \quad (1)$$

where $x(t) \in \mathbb{R}^n$, $t \geq 0$, $u(t) \in \mathbb{R}^m$, $t \geq 0$, $f : \mathbb{R}^n \to \mathbb{R}^n$ is locally Lipschitz continuous and satisfies $f(0) = 0$, $G : \mathbb{R}^n \to \mathbb{R}^{n\times m}$ is continuous, and $u : [0, \infty) \to \mathbb{R}^m$ is piecewise continuous.

Definition 2.3 and Proposition 2.1 are needed for the main results of this paper.

Definition 2.3: The nonlinear dynamical system given by (1) is *nonnegative* if for every $x(0) \in \overline{\mathbb{R}}_+^n$ and $u(t) \geq\geq 0$, $t \geq 0$, the solution $x(t)$, $t \geq 0$, to (1) is nonnegative.

Proposition 2.1 ([7]): The nonlinear dynamical system given by (1) is nonnegative if $f : \mathbb{R}^n \to \mathbb{R}^n$ is essentially nonnegative and $G(x) \geq\geq 0$, $x \in \overline{\mathbb{R}}_+^n$.

It follows from Proposition 2.1 that a nonnegative input signal $G(x(t))u(t)$, $t \geq 0$, is sufficient to guarantee the nonnegativity of the state of (1).

III. Partial Boundedness and Partial Ultimate Boundedness

In this section, we present Lyapunov-like theorems for *partial boundedness* and *partial ultimate boundedness* of nonlinear dynamical systems. These notions allow us to develop less conservative ultimate bounds for neuroadaptive controllers as compared to ultimate bounds derived using classical boundedness and ultimate boundedness notions [26]. Specifically, consider the nonlinear autonomous interconnected dynamical system

$$\dot{x}_1(t) = f_1(x_1(t), x_2(t)) \quad x_1(0) = x_{10}, \qquad t \in \mathcal{I}_{x_{10},x_{20}} \quad (2)$$

$$\dot{x}_2(t) = f_2(x_1(t), x_2(t)) \quad x_2(0) = x_{20} \quad (3)$$

where $x_1 \in \mathcal{D}$, $\mathcal{D} \subseteq \mathbb{R}^{n_1}$ is an open set such that $0 \in \mathcal{D}$, $x_2 \in \mathbb{R}^{n_2}$, $f_1 : \mathcal{D} \times \mathbb{R}^{n_2} \to \mathbb{R}^{n_1}$ is such that, for every $x_2 \in \mathbb{R}^{n_2}$, $f_1(0, x_2) = 0$ and $f_1(\cdot, x_2)$ is locally Lipschitz continuous in x_1, $f_2 : \mathcal{D} \times \mathbb{R}^{n_2} \to \mathbb{R}^{n_2}$ is such that, for every $x_1 \in \mathcal{D}$, $f_2(x_1, \cdot)$ is locally Lipschitz continuous in x_2, and $\mathcal{I}_{x_{10},x_{20}} \triangleq [0, \tau_{x_{10},x_{20}})$, $0 < \tau_{x_{10},x_{20}} \leq \infty$, is the maximal interval of existence for the solution $(x_1(t), x_2(t))$, $t \in \mathcal{I}_{x_{10},x_{20}}$, to (2)

[1] In this paper, it is important to distinguish between a square nonnegative (respectively, positive) matrix and a nonnegative–definite (respectively, positive–definite) matrix.

and (3). Note that under the aforementioned assumptions the solution $(x_1(t), x_2(t))$ to (2) and (3) exists and is unique over $\mathcal{I}_{x_{10},x_{20}}$. For Definition 3.1, we assume that $\mathcal{I}_{x_{10},x_{20}} = [0,\infty)$.

Definition 3.1:

1) The nonlinear dynamical system (2) and (3) is *bounded with respect to x_1 uniformly in x_{20}* if there exists $\gamma > 0$ such that, for every $\delta \in (0,\gamma)$, there exists $\varepsilon = \varepsilon(\delta) > 0$ such that $\|x_{10}\| < \delta$ implies $\|x_1(t)\| < \varepsilon$, $t \geq 0$. The nonlinear dynamical system (2) and (3) is *globally bounded with respect to x_1 uniformly in x_{20}* if, for every $\delta \in (0,\infty)$, there exists $\varepsilon = \varepsilon(\delta) > 0$ such that $\|x_{10}\| < \delta$ implies $\|x_1(t)\| < \varepsilon$, $t \geq 0$.
2) The nonlinear dynamical system (2) and (3) is *ultimately bounded with respect to x_1 uniformly in x_{20} with ultimate bound ε* if there exists $\gamma > 0$ such that, for every $\delta \in (0,\gamma)$, there exists $T = T(\delta,\varepsilon) > 0$ such that $\|x_{10}\| < \delta$ implies $\|x_1(t)\| < \varepsilon$, $t \geq T$. The nonlinear dynamical system (2) and (3) is *globally ultimately bounded with respect to x_1 uniformly in x_{20} with ultimate bound ε* if, for every $\delta \in (0,\infty)$, there exists $T = T(\delta,\varepsilon) > 0$ such that $\|x_{10}\| < \delta$ implies $\|x_1(t)\| < \varepsilon$, $t \geq T$.

Note that if a nonlinear dynamical system is (globally) bounded with respect to x_1 uniformly in x_{20}, then there exists $\varepsilon > 0$ such that it is (globally) ultimately bounded with respect to x_1 uniformly in x_{20} with an ultimate bound ε. Conversely, if a nonlinear dynamical system is (globally) ultimately bounded with respect to x_1 uniformly in x_{20} with an ultimate bound ε, then it is (globally) bounded with respect to x_1 uniformly in x_{20}. The following results present Lyapunov-like theorems for partial boundedness and partial ultimate boundedness. For these results, define $\dot{V}(x_1,x_2) \triangleq V'(x_1,x_2)f(x_1,x_2)$, where $f(x_1,x_2) \triangleq [f_1^{\mathrm{T}}(x_1,x_2), f_2^{\mathrm{T}}(x_1,x_2)]^{\mathrm{T}}$ and $V : \mathcal{D} \times \mathbb{R}^{n_2} \to \mathbb{R}$ is a given continuously differentiable function. Furthermore, let $\mathcal{B}_\delta(x)$, $x \in \mathbb{R}^n$, $\delta > 0$, denote the open ball *centered* at x with *radius* δ, let $\overline{\mathcal{B}}_\delta(x)$ denote the closure of $\mathcal{B}_\delta(x)$, and recall the definitions of class $\mathcal{K}$, class $\mathcal{K}_\infty$, and class $\mathcal{KL}$ functions [26].

Theorem 3.1: Consider the nonlinear dynamical system (2) and (3). Assume there exist a continuously differentiable function $V : \mathcal{D} \times \mathbb{R}^{n_2} \to \mathbb{R}$ and class $\mathcal{K}$ functions $\alpha(\cdot)$ and $\beta(\cdot)$ such that

$$\alpha(\|x_1\|) \leq V(x_1,x_2) \leq \beta(\|x_1\|), \qquad x_1 \in \mathcal{D}; \qquad x_2 \in \mathbb{R}^{n_2} \tag{4}$$

$$\dot{V}(x_1,x_2) \leq 0, \qquad x_1 \in \mathcal{D}; \qquad \|x_1\| \geq \mu; \qquad x_2 \in \mathbb{R}^{n_2} \tag{5}$$

where $\mu > 0$ is such that $\mathcal{B}_{\alpha^{-1}(\eta)}(0) \subset \mathcal{D}$ for some $\eta \geq \beta(\mu)$. Then, the nonlinear dynamical system (2) and (3) is bounded with respect to x_1 uniformly in x_{20}. Furthermore, for every $\delta \in (0,\gamma)$, $x_{10} \in \overline{\mathcal{B}}_\delta(0)$ implies that $\|x_1(t)\| \leq \varepsilon$, where

$$\varepsilon(\delta) \triangleq \begin{cases} \alpha^{-1}(\beta(\delta)), & \delta \in (\mu,\gamma) \\ \alpha^{-1}(\eta), & \delta \in (0,\mu] \end{cases} \tag{6}$$

and $\gamma \triangleq \sup\{r > 0 : \mathcal{B}_{\alpha^{-1}(\beta(r))}(0) \subset \mathcal{D}\}$. If, in addition, $\mathcal{D} = \mathbb{R}^{n_1}$ and $\alpha(\cdot)$ is a class $\mathcal{K}_\infty$ function, then the nonlinear dynamical system (2) and (3) is globally bounded with respect to x_1 uniformly in x_{20}, and for every $x_{10} \in \mathbb{R}^{n_1}$, $\|x_1(t)\| \leq \varepsilon$, $t \geq 0$, where ε is given by (6) with $\delta = \|x_{10}\|$.

Proof: First, let $\delta \in (0,\mu]$ and assume $\|x_{10}\| \leq \delta$. If $\|x_1(t)\| \leq \mu, t \geq 0$, then it follows from (4) that $\|x_1(t)\| \leq \mu \leq \alpha^{-1}(\beta(\mu)) \leq \alpha^{-1}(\eta)$, $t \geq 0$. Alternatively, if there exists $T > 0$ such that $\|x_1(T)\| > \mu$, then it follows from the continuity of $x_1(\cdot)$ that there exists $\tau < T$ such that $\|x_1(\tau)\| = \mu$ and $\|x_1(t)\| \geq \mu$, $t \in [\tau, T]$. Hence, it follows from (4) and (5) that

$$\begin{aligned} \alpha(\|x_1(T)\|) &\leq V(x_1(T),x_2(T)) \\ &\leq V(x_1(\tau),x_2(\tau)) \leq \beta(\mu) \leq \eta \end{aligned} \tag{7}$$

which implies that $\|x_1(T)\| \leq \alpha^{-1}(\eta)$. Next, let $\delta \in (\mu,\gamma)$ and assume $x_{10} \in \overline{\mathcal{B}}_\delta(0)$ and $\|x_{10}\| > \mu$. Now, for every $\hat{t} > 0$ such that $\|x_1(t)\| \geq \mu$, $t \in [0,\hat{t}]$, it follows from (4) and (5) that

$$\alpha(\|x_1(t)\|) \leq V(x_1(t),x_2(t)) \leq V(x_{10},x_{20}) \leq \beta(\delta), \qquad t \geq 0$$

which implies that $\|x_1(t)\| \leq \alpha^{-1}(\beta(\delta))$, $t \in [0,\hat{t}]$. Next, if there exists $T > 0$ such that $\|x_1(T)\| \leq \mu$, then it follows as in the proof of the first case given previously that $\|x_1(t)\| \leq \alpha^{-1}(\eta), t \geq T$. Hence, if $x_{10} \in \mathcal{B}_\delta(0) \setminus \mathcal{B}_\mu(0)$, then $\|x_1(t)| \leq \alpha^{-1}(\beta(\delta))$, $t \geq 0$. Finally, if $\mathcal{D} = \mathbb{R}^{n_1}$ and $\alpha(\cdot)$ is a class $\mathcal{K}_\infty$ function it follows that $\beta(\cdot)$ is a class $\mathcal{K}_\infty$ function, and hence, $\gamma = \infty$. Hence, the nonlinear dynamical system (2) and (3) is globally bounded with respect to x_1 uniformly in x_{20}. □

Theorem 3.2: Consider the nonlinear dynamical system (2) and (3). Assume there exist a continuously differentiable function $V : \mathcal{D} \times \mathbb{R}^{n_2} \to \mathbb{R}$ and class $\mathcal{K}$ functions $\alpha(\cdot)$ and $\beta(\cdot)$ such that (4) holds. Furthermore, assume that there exists a continuous, positive–definite function $W : \mathcal{D} \to \mathbb{R}$ such that $W(x_1) > 0$, $\|x_1\| > \mu$, and

$$\dot{V}(x_1,x_2) \leq -W(x_1), \qquad x_1 \in \mathcal{D}; \qquad \|x_1\| > \mu; \qquad x_2 \in \mathbb{R}^{n_2} \tag{8}$$

where $\mu > 0$ is such that $\mathcal{B}_{\alpha^{-1}(\eta)}(0) \subset \mathcal{D}$ for some $\eta > \beta(\mu)$. Then, the nonlinear dynamical system (2) and (3) is ultimately bounded with respect to x_1 uniformly in x_{20} with ultimate bound $\varepsilon \triangleq \alpha^{-1}(\eta)$. Furthermore, $\limsup_{t\to\infty} \|x_1(t)\| \leq \alpha^{-1}(\beta(\mu))$. If, in addition, $\mathcal{D} = \mathbb{R}^n$ and $\alpha(\cdot)$ is a class $\mathcal{K}_\infty$ function, then the nonlinear dynamical system (2) and (3) is globally ultimately bounded with respect to x_1 uniformly in x_{20} with ultimate bound ε.

Proof: First, let $\delta \in (0,\mu]$ and assume $\|x_{10}\| \leq \delta$. As in the proof of Theorem 3.1, it follows that $\|x_1(t)\| \leq \alpha^{-1}(\eta) = \varepsilon$, $t \geq 0$. Next, let $\delta \in (\mu,\gamma)$, where $\gamma \triangleq \sup\{r > 0 : \mathcal{B}_{\alpha^{-1}(\beta(r))}(0) \subset \mathcal{D}\}$ and assume $x_{10} \in \mathcal{B}_\delta(0)$ and $\|x_{10}\| > \mu$. In this case, it follows from Theorem 3.1 that $\|x_1(t)\| \leq \alpha^{-1}(\beta(\delta))$, $t \geq 0$. Suppose, *ad absurdum*, $\|x_1(t)\| \geq \beta^{-1}(\eta)$, $t \geq 0$, or, equivalently, $x_1(t) \in \mathcal{O} \triangleq \mathcal{B}_{\alpha^{-1}(\beta(\delta))}(0) \setminus \mathcal{B}_{\beta^{-1}(\eta)}(0)$, $t \geq 0$. Since $\overline{\mathcal{O}}$ is compact, $W(\cdot)$ is continuous, and $W(x_1) > 0$, $\|x_1\| \geq \beta^{-1}(\eta) > \mu$, it follows from Weierstrass' theorem [27, p. 154] that $k \triangleq \min_{x_1 \in \overline{\mathcal{O}}} W(x_1) > 0$ exists. Hence, it follows from (8) that:

$$V(x_1(t),x_2(t)) \leq V(x_{10},x_{20}) - kt, \qquad t \geq 0 \tag{9}$$

which implies that

$$\alpha(\|x_1(t)\|) \leq \beta(\|x_{10}\|) - kt \leq \beta(\delta) - kt, \qquad t \geq 0. \quad (10)$$

Now, letting $t > \beta(\delta)/k$ it follows that $\alpha(\|x_1(t)\|) < 0$, which is a contradiction. Hence, there exists $T = T(\delta, \eta) > 0$ such that $\|x_1(T)\| < \beta^{-1}(\eta)$. Thus, it follows from Theorem 3.1 that $\|x_1(t)\| \leq \alpha^{-1}(\beta(\beta^{-1}(\eta))) = \alpha^{-1}(\eta)$, $t \geq T$, which proves that the nonlinear dynamical system (2) and (3) is ultimately bounded with respect to x_1 uniformly in x_{20} with ultimate bound $\varepsilon = \alpha^{-1}(\eta)$. Furthermore, $\limsup_{t\to\infty} \|x_1(t)\| \leq \alpha^{-1}(\beta(\mu))$. Finally, if $\mathcal{D} = \mathbb{R}^{n_1}$ and $\alpha(\cdot)$ is a class $\mathcal{K}_\infty$ function it follows that $\beta(\cdot)$ is a class $\mathcal{K}_\infty$ function, and hence, $\gamma = \infty$. Hence, the nonlinear dynamical system (2) and (3) is globally ultimately bounded with respect to x_1 uniformly in x_{20} with ultimate bound ε. □

The following result on ultimate boundedness of interconnected systems is needed for the main theorem in this paper. For this result, recall the definition of input-to-state stability given in [26].

Proposition 3.1: Consider the nonlinear interconnected dynamical system (2) and (3). If (3) is input-to-state stable with x_1 viewed as the input and (2) and (3) is ultimately bounded with respect to x_1 uniformly in x_{20}, then the solution $(x_1(t), x_2(t))$, $t \geq 0$, of the interconnected dynamical system (2) and (3) is ultimately bounded.

Proof: Since (2) and (3) is ultimately bounded with respect to x_1 (uniformly in x_{20}), there exist positive constants ε and $T = T(\delta, \varepsilon)$ such that $\|x_1(t)\| < \varepsilon$, $t \geq T$. Furthermore, since (3) is input-to-state stable with x_1 viewed as the input, it follows that $x_2(T)$ is finite, and hence, there exist a class $\mathcal{KL}$ function $\eta(\cdot,\cdot)$ and a class $\mathcal{K}$ function $\gamma(\cdot)$ such that

$$\begin{aligned}\|x_2(t)\| &\leq \eta(\|x_2(T)\|, t-T) + \gamma\left(\sup_{T\leq\tau\leq t}\|x_1(\tau)\|\right)\\ &= \eta(\|x_2(T)\|, t-T) + \gamma(\varepsilon)\\ &\leq \eta(\|x_2(T)\|, 0) + \gamma(\varepsilon), \qquad t \geq T \end{aligned} \quad (11)$$

which proves that the solution $(x_1(t), x_2(t))$, $t \geq 0$, to (2) and (3) is ultimately bounded. □

IV. Neural Adaptive Output Feedback Control for Nonlinear Nonnegative Uncertain Systems

In this section, we consider the problem of characterizing neural adaptive dynamic output feedback control laws for nonlinear nonnegative and compartmental uncertain dynamical systems to achieve *set-point* regulation in the nonnegative orthant. Specifically, consider the controlled square nonlinear uncertain dynamical system $\mathcal{G}$ given by

$$\dot{x}(t) = f(x(t)) + G(x(t))\,u(t), \qquad x(0) = x_0; \qquad t \geq 0 \quad (12)$$

$$y(t) = h(x(t)) \quad (13)$$

where $x(t) \in \mathbb{R}^n$, $t \geq 0$, is the state vector, $u(t) \in \mathbb{R}^m$, $t \geq 0$, is the control input, $y(t) \in \mathbb{R}^m$, $t \geq 0$, is the system output, $f : \mathbb{R}^n \to \mathbb{R}^n$ is essentially nonnegative but otherwise unknown and satisfies $f(0) = 0$, $G : \mathbb{R}^n \to \mathbb{R}^{n\times m}$ is an unknown nonnegative input matrix function, and $h : \mathbb{R}^n \to \mathbb{R}^m$ is a nonnegative output function and satisfies $h(0) = 0$. We assume that $f(\cdot)$, $G(\cdot)$, and $h(\cdot)$ are smooth (at least C^n mappings) and the control input $u(\cdot)$ in (12) is restricted to the class of *admissible controls* consisting of measurable functions such that $u(t) \in \mathbb{R}^m$, $t \geq 0$.

As discussed in Section I, control (source) inputs of drug delivery systems for physiological and pharmacological processes are usually constrained to be nonnegative as are the system states. Hence, in this paper, we develop neuroadaptive dynamic output feedback control laws for nonnegative systems with nonnegative control inputs. Specifically, for a given desired set point $y_{\mathrm{d}} \in \overline{\mathbb{R}}_+^m$ and for a given $\varepsilon > 0$, our aim is to design a nonnegative control input $u(t)$, $t \geq 0$, predicated on the system measurement $y(t)$, $t \geq 0$, such that $\|y(t) - y_{\mathrm{d}}\| < \varepsilon$ for all $t \geq T$, where $T \in [0, \infty)$, and $x(t) \geq\geq 0$, $t \geq 0$, for all $x_0 \in \overline{\mathbb{R}}_+^n$.

In this paper, we assume that for the nonlinear dynamical systems (12) and (13), the conditions for the existence of a globally defined diffeomorphism transforming (12) and (13) into a normal form [28], [29] are satisfied. Specifically, we assume that there exist a global diffeomorphism $\mathcal{T} : \mathbb{R}^n \to \mathbb{R}^n$ and C^n functions $f_\xi : \mathbb{R}^r \times \mathbb{R}^{n-r} \to \mathbb{R}^r$ and $f_z : \mathbb{R}^r \times \mathbb{R}^{n-r} \to \mathbb{R}^{n-r}$ such that, in the coordinates

$$\begin{bmatrix}\xi\\ z\end{bmatrix} \triangleq \mathcal{T}(x) \quad (14)$$

where $\xi \triangleq [y_1, \dot{y}_1, \cdots, y_1^{(r_1-2)}, \cdots, y_m, \dot{y}_m, \cdots, y_m^{(r_m-2)}; y_1^{(r_1-1)}, \cdots, y_m^{(r_m-1)}] \in \mathbb{R}^r$, $y_i^{(r_i)}$ denotes the r_ith derivative of y_i, r_i denotes the relative degree of $\mathcal{G}$ with respect to the output y_i, $z \in \mathbb{R}^{n-r}$, and $r \triangleq r_1 + \cdots + r_m$ is the (vector) relative degree of $\mathcal{G}$, the nonlinear dynamical system $\mathcal{G}$ given by (12) and (13) is equivalent to

$$\begin{aligned}\dot{\xi}(t) &= f_\xi(\xi(t), z(t)) + G_\xi(\xi(t), z(t))\,u(t),\\ &\qquad \xi(0) = \xi_0; \qquad t \geq 0 \end{aligned} \quad (15)$$

$$\dot{z}(t) = f_z(\xi(t), z(t)), \qquad z(0) = z_0 \quad (16)$$

$$y(t) = C\xi(t) \quad (17)$$

where $\xi(t) \in \mathbb{R}^r$, $t \geq 0$, $z(t) \in \mathbb{R}^{n-r}$, $t \geq 0$

$$f_\xi(\xi, z) = A\xi + \tilde{f}_{\mathrm{u}}(\xi, z) \quad G_\xi(\xi, z) = \begin{bmatrix}0_{(r-m)\times m}\\ \hat{G}(\tilde{x})\end{bmatrix} \quad (18)$$

$$A = \begin{bmatrix}A_0\\ \hat{A}\end{bmatrix} \quad \tilde{f}_{\mathrm{u}}(\xi, z) = \begin{bmatrix}0_{(r-m)\times 1}\\ f_{\mathrm{u}}(\tilde{x})\end{bmatrix} \quad (19)$$

$\tilde{x} \triangleq [\xi^{\mathrm{T}}, z^{\mathrm{T}}]^{\mathrm{T}}$, $A_0 \in \mathbb{R}^{(r-m)\times r}$ is a known matrix of 0s and 1s capturing the multivariable controllable canonical form representation [30], $\hat{A} \in \mathbb{R}^{m\times r}$ is such that A is asymptotically stable, $f_{\mathrm{u}} : \mathbb{R}^n \to \mathbb{R}^m$ is an unknown function and satisfies $f_{\mathrm{u}}(0) = 0$, $C \in \mathbb{R}^{m\times r}$ is a known matrix of 0s and 1s capturing the system output, and $\hat{G} : \mathbb{R}^n \to \mathbb{R}^{m\times m}$ is an unknown matrix function such that $\det \hat{G}(\tilde{x}) \neq 0$, $\tilde{x} \in \mathbb{R}^n$. Furthermore, we assume that for a given $y_{\mathrm{d}} \in \overline{\mathbb{R}}_+^m$ there exist $z_{\mathrm{e}} \in \mathbb{R}^{n-r}$ and $u_{\mathrm{e}} \in \overline{\mathbb{R}}_+^m$ such that $x_{\mathrm{e}} \triangleq \mathcal{T}^{-1}(\tilde{x}_{\mathrm{e}}) \geq\geq 0$ and

$$0 = f_\xi(\xi_{\mathrm{e}}, z_{\mathrm{e}}) + G_\xi(\xi_{\mathrm{e}}, z_{\mathrm{e}})u_{\mathrm{e}} \quad (20)$$

$$0 = f_z(\xi_{\mathrm{e}}, z_{\mathrm{e}}) \quad (21)$$

where $\tilde{x}_{\mathrm{e}} \triangleq [\xi_{\mathrm{e}}^{\mathrm{T}}, z_{\mathrm{e}}^{\mathrm{T}}]^{\mathrm{T}}$ and ξ_{e} is given with $y_i = y_{\mathrm{d}i}$, $i = 1, \cdots, m$, and $\dot{y}_i = \cdots = y_i^{(r_i-1)} = 0$, $i = 1, \cdots, m$.

To ensure that for a bounded state $\xi(t)$, $t \geq 0$, the dynamics given by (16) are bounded, we assume that (16) is input-to-state stable at $z(t) \equiv z_{\mathrm{e}}$ with $\xi(t) - \xi_{\mathrm{e}}$ viewed as the input; that is, there exist a class $\mathcal{KL}$ function $\eta(\cdot, \cdot)$ and a class $\mathcal{K}$ function $\gamma(\cdot)$ such that

$$\|z(t) - z_{\mathrm{e}}\| \leq \eta(\|z_0 - z_{\mathrm{e}}\|, t) + \gamma\left(\sup_{0 \leq \tau \leq t} \|\xi(\tau) - \xi_{\mathrm{e}}\|\right), \qquad t \geq 0 \quad (22)$$

where $\|\cdot\|$ denotes the Euclidean vector norm. Unless otherwise stated, henceforth we use $\|\cdot\|$ to denote the Euclidean vector norm. Note that $(\xi_{\mathrm{e}}, z_{\mathrm{e}}) \in \mathbb{R}^r \times \mathbb{R}^{n-r}$ is an equilibrium point of (15) and (16) if and only if there exists $u_{\mathrm{e}} \in \overline{\mathbb{R}}_+^m$ such that (20) and (21) hold.

Finally, we assume that the functions $f_{\mathrm{u}}(\mathcal{T}(x)) - f_{\mathrm{u}}(\mathcal{T}(x_{\mathrm{e}})) - \hat{G}(\mathcal{T}(x_{\mathrm{e}}))u_{\mathrm{e}}$ and $\hat{G}(\mathcal{T}(x)) - \hat{B}$, where $\hat{B} \in \mathbb{R}^{m \times m}$, can be approximated over a compact set $\mathcal{D}_{\mathrm{c}} \subset \overline{\mathbb{R}}_+^n$ by a linear in the parameters neural network up to a desired accuracy. In this case, there exist $\varepsilon_1 : \mathbb{R}^n \to \mathbb{R}^m$ and $\varepsilon_2 : \mathbb{R}^n \to \mathbb{R}^{m \times m}$ such that $\|\varepsilon_1(x)\| < \varepsilon_1^*$ and $\|\varepsilon_2(x)|_{\mathrm{F}} < \varepsilon_2^*$, $x \in \mathcal{D}_{\mathrm{c}}$, where $\varepsilon_1^* > 0$ and $\varepsilon_2^* > 0$, and

$$f_{\mathrm{u}}(\mathcal{T}(x)) - f_{\mathrm{u}}(\mathcal{T}(x_{\mathrm{e}})) - \hat{G}(\mathcal{T}(x_{\mathrm{e}}))\, u_{\mathrm{e}} = W_1^{\mathrm{T}} \hat{\sigma}_1(x) + \varepsilon_1(x) \quad (23)$$

$$\hat{G}(\mathcal{T}(x)) - \hat{B} = W_2^{\mathrm{T}} [I_m \otimes \hat{\sigma}_2(x)] + \varepsilon_2(x) \quad (24)$$

for all $x \in \mathcal{D}_{\mathrm{c}}$, where $W_1 \in \mathbb{R}^{s_1 \times m}$ and $W_2 \in \mathbb{R}^{ms_2 \times m}$ are optimal *unknown* (constant) weights that minimize the approximation errors over $\mathcal{D}_{\mathrm{c}}$, $\hat{\sigma}_1 : \mathbb{R}^n \to \mathbb{R}^{s_1}$ and $\hat{\sigma}_2 : \mathbb{R}^n \to \mathbb{R}^{s_2}$ are sets of basis functions such that each component of $\hat{\sigma}_1(\cdot)$ and $\hat{\sigma}_2(\cdot)$ takes values between 0 and 1, and $\varepsilon_1(\cdot)$ and $\varepsilon_2(\cdot)$ are the modeling errors. Note that $s_1 + s_2$ denotes the total number of basis functions or, equivalently, the number of nodes of the neural network.

Since $f_{\mathrm{u}}(\cdot)$ and $\hat{G}(\cdot)$ are continuous, we can choose $\hat{\sigma}_1(\cdot)$ and $\hat{\sigma}_2(\cdot)$ from a linear space $\mathcal{X}$ of continuous functions that forms an algebra and separates points in $\mathcal{D}_{\mathrm{c}}$. In this case, it follows from the Stone–Weierstrass theorem [27, p. 212] that $\mathcal{X}$ is a dense subset of the set of continuous functions on $\mathcal{D}_{\mathrm{c}}$. Now, as is the case in the standard neuroadaptive control literature [18], we can construct the signal $u_{\mathrm{ad}} = F(\hat{W}_1, \hat{W}_2, \hat{\sigma}_1(x), \hat{\sigma}_2(x))$, where $F : \mathbb{R}^{s_1 \times m} \times \mathbb{R}^{ms_2 \times m} \times \mathbb{R}^{s_1} \times \mathbb{R}^{s_2} \to \mathbb{R}^m$, involving the estimates of the optimal weights and basis functions as our adaptive control signal.

In order to develop an *output* feedback neural network, we use the recent approach developed in [31] for reconstructing the system states via the system delayed inputs and outputs. Specifically, we use a *memory unit* as a particular form of a tapped delay line that takes a scalar time-series input and provides an $(2mn - r)$-dimensional vector output consisting of the present values of the system outputs and system inputs, and their $2(n-1)m - r$ delayed values given by

$$\begin{aligned}\zeta(t) \triangleq [&y_1(t), y_1(t-d), \cdots, y_1(t-(n-1)d), \cdots, \\ &y_m(t), y_m(t-d), \cdots, y_m(t-(n-1)d); \\ &u_1(t), u_1(t-d), \cdots, u_1(t-(n-r_1-1)d), \cdots, \\ &u_m(t), u_m(t-d), \cdots, u_m(t-(n-r_m-1)d)]^{\mathrm{T}}, \\ &t \geq 0 \end{aligned} \quad (25)$$

where $d > 0$.

For the statement of our main result, define the projection operator $\mathrm{Proj}(\tilde{W}, Y)$ given by

$$\mathrm{Proj}(\tilde{W}, Y) \triangleq \begin{cases} Y, & \text{if } \mu(\tilde{W}) < 0 \\ Y, & \text{if } \mu(\tilde{W}) \geq 0 \text{ and } \mu'(\tilde{W})Y \leq 0 \\ Y - \frac{\mu'^{\mathrm{T}}(\tilde{W})\mu'(\tilde{W})Y}{\mu'(\tilde{W})\mu'^{\mathrm{T}}(\tilde{W})}\mu(\tilde{W}), & \text{otherwise} \end{cases} \quad (26)$$

where $\tilde{W} \in \mathbb{R}^{s \times m}$, $Y \in \mathbb{R}^{n \times m}$, $\mu(\tilde{W}) \triangleq ((\mathrm{tr}\tilde{W}^{\mathrm{T}}\tilde{W} - \tilde{w}_{\max}^2)/\varepsilon_{\tilde{W}})$, $\tilde{w}_{\max} \in \mathbb{R}$ is the norm bound imposed on $\tilde{W}$, and $\varepsilon_{\tilde{W}} > 0$. Note that for a given matrix $\tilde{W} \in \mathbb{R}^{s \times m}$ and $Y \in \mathbb{R}^{n \times m}$, it follows:

$$\begin{aligned}&\mathrm{tr}\left[(\tilde{W} - W)^{\mathrm{T}}\left(\mathrm{Proj}(\tilde{W}, Y) - Y\right)\right] \\ &= \sum_{i=1}^{n} \left[\mathrm{col}_i(\tilde{W} - W)\right]^{\mathrm{T}} \\ &\quad \times \left[\mathrm{Proj}\left(\mathrm{col}_i(\tilde{W}), \mathrm{col}_i(Y)\right) - \mathrm{col}_i(Y)\right] \\ &\leq 0 \end{aligned} \quad (27)$$

where $\mathrm{col}_i(X)$ denotes the ith column of the matrix X.

Assumption 4.1: For a given $y_{\mathrm{d}} \in \overline{\mathbb{R}}_+^m$, assume there exist nonnegative vectors $x_{\mathrm{e}} \in \overline{\mathbb{R}}_+^n$ and $u_{\mathrm{e}} \in \overline{\mathbb{R}}_+^m$ such that

$$0 = f(x_{\mathrm{e}}) + G(x_{\mathrm{e}})u_{\mathrm{e}} \quad (28)$$

$$y_{\mathrm{d}} = h(x_{\mathrm{e}}). \quad (29)$$

Furthermore, assume that the equilibrium point x_{e} of (12) is globally asymptotically stable with $u(t) \equiv u_{\mathrm{e}}$. Finally, assume that there exists a global diffeomorphism $\mathcal{T} : \mathbb{R}^n \to \mathbb{R}^n$ such that $\mathcal{G}$ can be transformed into the normal form given by (15) and (16), and (16) is input-to-state stable at z_{e} with $\xi(t) - \xi_{\mathrm{e}}$ viewed as the input.

Consider the neural adaptive output feedback control law given by

$$u(t) = \begin{cases} \hat{u}(t), & \text{if } \hat{u}(t) \geq\geq 0 \\ 0, & \text{otherwise} \end{cases} \quad (30)$$

where

$$\hat{u}(t) = -\left(\hat{B} + \hat{W}_2^{\mathrm{T}}(t)\left[I_m \otimes \sigma_2(\zeta(t))\right]\right)^{-1} \hat{W}_1^{\mathrm{T}}(t)\sigma_1(\zeta(t)) \quad (31)$$

$\hat{B} \in \mathbb{R}^{m\times m}$ is nonsingular, $\zeta(t)$, $t \geq 0$, is given by (25), $\sigma_1 : \mathbb{R}^n \to \mathbb{R}^{s_1}$ and $\sigma_2 : \mathbb{R}^n \to \mathbb{R}^{s_2}$ are sets of basis functions such that each component of $\sigma_1(\cdot)$ and $\sigma_2(\cdot)$ takes values between 0 and 1, $\hat{W}_1(t) \in \mathbb{R}^{s_1\times m}$, $t \geq 0$, and $\hat{W}_2(t) \in \mathbb{R}^{ms_2\times m}$, $t \geq 0$. Here, the update laws satisfy

$$\dot{\hat{W}}_1(t) = Q_1 \mathrm{Proj}\Big[\hat{W}_1(t), -\sigma_1(\zeta(t))\xi_{\mathrm{c}}^{\mathrm{T}}(t)\tilde{P}B_0\Big]$$
$$\hat{W}_1(0) = \hat{W}_{10}, \qquad t \geq 0 \tag{32}$$
$$\dot{\hat{W}}_2(t) = Q_2 \mathrm{Proj}\Big[\hat{W}_2(t), -[I_m \otimes \sigma_2(\zeta(t))]\, u(t)\xi_{\mathrm{c}}^{\mathrm{T}}(t)\tilde{P}B_0\Big]$$
$$\hat{W}_2(0) = \hat{W}_{20} \tag{33}$$

where $Q_1 \in \mathbb{R}^{m\times m}$ and $Q_2 \in \mathbb{R}^{m\times m}$ are positive–definite matrices, $\tilde{P} \in \mathbb{R}^{r\times r}$ is a positive–definite solution of the Lyapunov equation

$$0 = (A - LC)^{\mathrm{T}}\tilde{P} + \tilde{P}(A - LC) + \tilde{R}, \qquad \tilde{R} > 0 \tag{34}$$

and $\xi_{\mathrm{c}}(t)$, $t \geq 0$, is the solution to the estimator dynamics

$$\dot{\xi}_{\mathrm{c}}(t) = A\xi_{\mathrm{c}}(t) + L\left(y(t) - y_{\mathrm{c}}(t) - y_{\mathrm{d}}\right),$$
$$\xi_{\mathrm{c}}(0) = \xi_{\mathrm{c}0}; \qquad t \geq 0 \tag{35}$$
$$y_{\mathrm{c}}(t) = C\xi_{\mathrm{c}}(t) \tag{36}$$

where $\xi_{\mathrm{c}}(t) \in \mathbb{R}^r$, $t \geq 0$, $A \in \mathbb{R}^{r\times r}$ is given by (19), $L \in \mathbb{R}^{r\times m}$ is such that $A - LC$ is asymptotically stable, and $B_0 \triangleq [0_{m\times(r-m)}, I_m]^{\mathrm{T}}$.

Theorem 4.1: Consider the nonlinear uncertain dynamical system $\mathcal{G}$ given by (12) and (13) with $u(t)$, $t \geq 0$, given by (30). Assume Assumption 4.1 holds. Then, there exists a compact positively invariant set $\mathcal{D}_\alpha \subset \mathbb{R}^n \times \mathbb{R}^r \times \mathbb{R}^{s_1\times m} \times \mathbb{R}^{ms_2\times m}$ such that $(x_{\mathrm{e}}, 0, W_1, W_2) \in \mathcal{D}_\alpha$, where $W_1 \in \mathbb{R}^{s_1\times m}$ and $W_2 \in \mathbb{R}^{ms_2\times m}$, and the solution $(x(t), \xi_{\mathrm{c}}(t), \hat{W}_1(t), \hat{W}_2(t))$, $t \geq 0$, of the closed-loop system given by (12), (30), (32), (33), (35), and (36) is ultimately bounded for all $(x(0), \xi_{\mathrm{c}}(0), \hat{W}_1(0), \hat{W}_2(0)) \in \mathcal{D}_\alpha$ with ultimate bound $\|y(t) - y_{\mathrm{d}}\|^2 < \varepsilon$, $t \geq T$, where

$$\varepsilon > \Bigg[\left(\sqrt{\frac{\nu}{\lambda_{\min}(RP^{-1})}} + \alpha_1\right)^2 + \left(\sqrt{\frac{\nu}{\lambda_{\min}(\tilde{R}\tilde{P}^{-1})}} + \alpha_2\right)^2 + \lambda_{\max}\left(Q_1^{-1}\right)\hat{w}_{1\max}^2 + \lambda_{\max}\left(Q_2^{-1}\right)\hat{w}_{2\max}^2\Bigg]^{\frac{1}{2}} \tag{37}$$

$$\nu \triangleq \frac{\alpha_1^2}{\lambda_{\min}(RP^{-1})} + \frac{\alpha_2^2}{\lambda_{\min}(\tilde{R}\tilde{P}^{-1})} \tag{38}$$

$$\alpha_1 \triangleq [\sqrt{s_1}\hat{w}_{1\max} + \sqrt{ms_2}\hat{w}_{2\max}u^*]\left\|P^{-1/2}(P + \tilde{P})B_0\right\| + (2\sqrt{s_1}\hat{w}_{1\max} + \sqrt{ms_2}\hat{w}_{2\max}u^* + (\varepsilon_1^* + \varepsilon_2^* u^*)) \times \|P^{1/2}B_0\| \tag{39}$$

$$\alpha_2 \triangleq [2\sqrt{s_1}\hat{w}_{1\max} + \sqrt{ms_2}\hat{w}_{2\max}u^* + (\varepsilon_1^* + \varepsilon_2^* u^*)] \times \|\tilde{P}^{1/2}B_0\| \tag{40}$$

$u^* \triangleq \sup_{t\geq 0}\|u(t)\|$, $\hat{w}_{i\max}$, $i = 1, 2$, are norm bounds imposed on $\hat{W}_i$, and $\tilde{P} \in \mathbb{R}^{r\times r}$ and $P \in \mathbb{R}^{r\times r}$ are the positive–definite solutions of the Lyapunov equations (34) and

$$0 = A^{\mathrm{T}}P + PA + R, \qquad R > 0. \tag{41}$$

Furthermore, $u(t) \geq\geq 0$, $t \geq 0$, and $x(t) \geq\geq 0$, $t \geq 0$, for all $x_0 \in \overline{\mathbb{R}}_+^n$.

Proof: The proof is given in the Appendix. □

A block diagram showing the neuroadaptive control architecture given in Theorem 4.1 is shown in Fig. 1. It is important to note that the existence of a global neural network approximator for an uncertain nonlinear map using the system outputs and inputs, and its delayed values cannot, in general, be established. In the proof of Theorem 4.1, as is common in the neural network literature, we assume that for a given arbitrarily large compact set $\mathcal{D}_{\mathrm{c}} \subset \mathbb{R}^n$, there exists an approximator for the unknown nonlinear map up to a desired accuracy. This assumption ensures that in the error space $\tilde{\mathcal{D}}_{\mathrm{e}}$ defined in the Appendix, there exists at least one Lyapunov level set such that the set inclusions invoked in the proof of Theorem 4.1 are satisfied. In the case where $f_{\mathrm{u}}(\cdot)$ and $\hat{G}(\cdot)$ are continuous on $\mathbb{R}^n$, it follows from the Stone–Weierstrass theorem that $f_{\mathrm{u}}(\cdot)$ and $\hat{G}(\cdot)$ can be approximated over an arbitrarily large compact set $\mathcal{D}_{\mathrm{c}}$ in the sense of (23) and (24). Furthermore, as shown in [31], if the system dynamics evolve on a bounded set, then there exist functions $\sigma_1(\cdot)$ and $\sigma_2(\cdot)$ such that $\hat{\sigma}_i(x) - \sigma_i(\zeta)$, $i = 1, 2$, are of order d and tend to zero as $d \to 0$. In this case, one recovers the actual bounds ε_1^* and ε_2^* in the neural network approximation associated with (23) and (24). Finally, we assume that $\hat{W}_2(0)$ is sufficiently close to the optimal weight W_2 so that $(\hat{B} + \hat{W}_2^{\mathrm{T}}(t)[I_m \otimes \sigma_2(\zeta(t))])^{-1}$ is nonsingular and bounded for all $t \geq 0$ so that there exists $u^* > 0$ such that $u^* \geq \|u(t)\|$, $t \geq 0$.

Implementing the neuroadaptive controller (31) requires a fixed-point iteration at each integration step, that is, the controller contains an algebraic constraint on u. For each choice of $\sigma_1(\cdot)$ and $\sigma_2(\cdot)$, this equation must be examined for solvability in terms of u. It is more practical to avoid this iteration by using one-step delayed values of u in calculating $\hat{u}$. Implementations using both approaches result in imperceptible differences in our numerical studies.

If the dynamical system $\mathcal{G}$ has an unknown dimension but with known relative degree, then Theorem 4.1 applies with a slight modification to the input vector of the neural network, that is, n in (25) should be replaced by a sufficiently large value that is greater than the largest possible system dimension. Furthermore, if the system is exponentially minimum phase at x_{e} with $C = I_m$ in (17) and constant control input u_{e}, then the neural adaptive output feedback controller can be significantly simplified. Specifically, the control law (30) with $\hat{u}(t) = -\hat{W}_1^{\mathrm{T}}(t)\sigma_1(y(t))$ and update law

$$\dot{\hat{W}}_1(t) = Q_1 \mathrm{Proj}\left[\hat{W}_1(t), -\sigma_1(y(t))\left(y(t) - y_{\mathrm{d}}\right)^{\mathrm{T}}\right]$$
$$\hat{W}_1(0) = \hat{W}_{10}, \qquad t \geq 0 \tag{42}$$

guarantee ultimate boundedness of the closed-loop system. In this case, the update law (33) and the estimator dynamics (35) and (36) are superfluous. For further details, see [21].

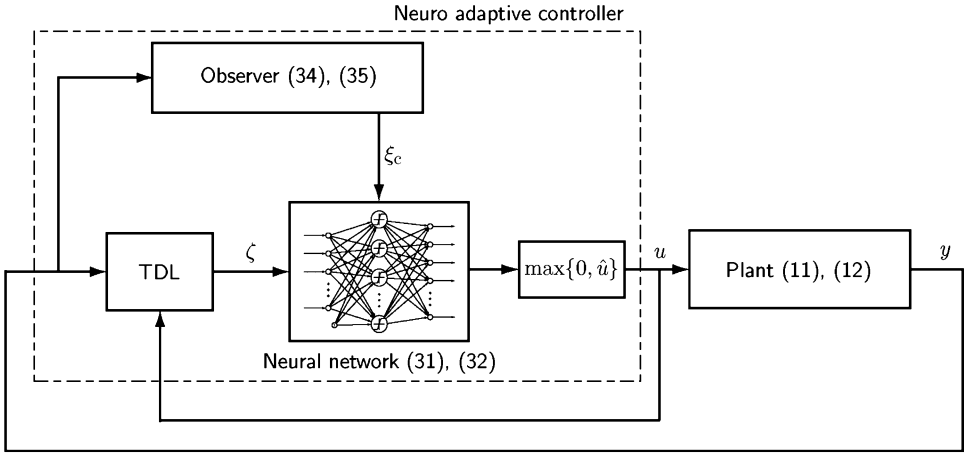

Fig. 1. Block diagram of the closed-loop system.

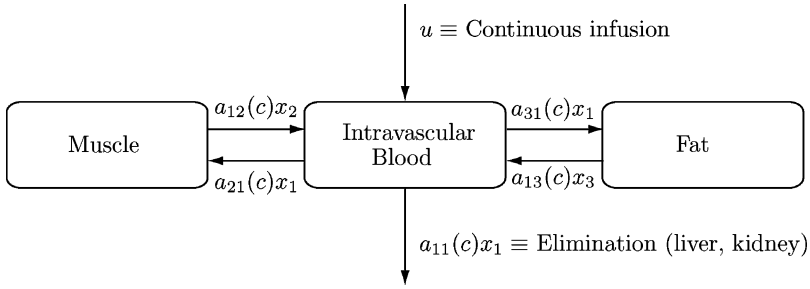

Fig. 2. Pharmacokinetic model for drug distribution during anesthesia.

In Theorem 4.1 we assumed that the equilibrium point x_e of (12) is globally asymptotically stable with $u(t) \equiv u_e$. In general, however, unlike linear nonnegative systems with asymptotically stable plant dynamics, a given set point $x_e \in \mathbb{R}^n_+$ for the nonlinear nonnegative dynamical system (12) may not be asymptotically stabilizable with a constant control $u(t) \equiv u_e \in \overline{\mathbb{R}}^m_+$. However, if $f(x)$ is homogeneous, cooperative, that is, the Jacobian matrix $\partial f(x)/\partial x$ is essentially nonnegative for all $x \in \overline{\mathbb{R}}^n_+$, the Jacobian matrix $\partial f(x)/\partial x$ is irreducible for all $x \in \overline{\mathbb{R}}^n_+$ [23], and the zero solution $x(t) \equiv 0$ of the undisturbed $(u(t) \equiv 0)$ system (12) is globally asymptotically stable, then the set point $x_e \in \mathbb{R}^n_+$ satisfying (20) and (21) is a unique equilibrium point with $u(t) \equiv u_e$ and is also asymptotically stable for all $x_0 \in \overline{\mathbb{R}}^n_+$ [32]. This implies that the solution $x(t) \equiv x_e$ to (12) with $u(t) \equiv u_e$ is asymptotically stable for all $x_0 \in \overline{\mathbb{R}}^n_+$.

V. Neuroadaptive Output Feedback Control for General Anesthesia

Almost all anesthetics are *myocardial* depressants, meaning that they decrease the strength of the contraction of the heart and lower *cardiac output*, that is, the volume of blood pumped by the heart per unit time. As a consequence, decreased cardiac output slows down redistribution kinetics, that is, the transfer of blood from the central compartments (heart, brain, kidney, and liver) to the peripheral compartments (muscle and fat). In addition, decreased cardiac output could increase drug concentrations in the central compartments, causing even more myocardial depression and further decrease in cardiac output. This instability can lead to overdosing that, at the very least, can delay recovery from anesthesia and, in the worst case, can result in respiratory and cardiovascular collapse. Alternatively, underdosing can result in patients psychologically traumatized by pain and awareness during surgery. Thus, control of drug effect is clinically important since overdosing or underdosing incur risk for the patient.

To illustrate the application of the neuroadaptive control framework presented in Section IV for general anesthesia we develop a model for the intravenous anesthetic propofol. The pharmacokinetics of propofol are described by the three-compartment model [7], [33] shown in Fig. 2, where x_1 denotes the mass of drug in the central compartment, which is the site for drug administration and is generally thought to be comprised of the *intravascular blood* volume (blood within arteries and veins) as well as *highly perfused* organs (organs with high ratios of blood flow to weight) such as the heart, brain, kidney, and liver. These organs receive a large fraction of the cardiac output. The remainder of the drug in the body is assumed to reside in two peripheral compartments, one identified with muscle and one with fat; the masses in these compartments are denoted by x_2 and x_3, respectively. These compartments receive less than 20% of the cardiac output.

A mass balance of the three-state compartmental model yields

$$\begin{aligned}\dot{x}_1(t) = &-\left[a_{11}\left(c(t)\right) + a_{21}\left(c(t)\right) + a_{31}\left(c(t)\right)\right] x_1(t) \\ &+ a_{12}\left(c(t)\right) x_2(t) + a_{13}\left(c(t)\right) x_3(t) + u(t), \\ &x_1(0) = x_{10}; \qquad t \geq 0 \end{aligned} \tag{43}$$

$$\dot{x}_2(t) = a_{21}\left(c(t)\right) x_1(t) - a_{12}\left(c(t)\right) x_2(t), \qquad x_2(0) = x_{20} \tag{44}$$

$$\dot{x}_3(t) = a_{31}\left(c(t)\right) x_1(t) - a_{13}\left(c(t)\right) x_3(t), \qquad x_3(0) = x_{30} \tag{45}$$

where $c(t) = x_1(t)/V_c$, V_c is the volume of the central compartment (about 15 l for a 70-kg patient), $a_{ij}(c)$, $i \neq j$, is the rate of transfer of drug from the jth compartment to the ith compartment, $a_{11}(c)$ is the rate of drug metabolism and elimination (metabolism typically occurs in the liver), and $u(t)$, $t \geq 0$, is the infusion rate of the anesthetic drug propofol into the central compartment. The transfer coefficients are assumed to be functions of the drug concentration c since it is well known that the pharmacokinetics of propofol are influenced by cardiac output [34] and, in turn, cardiac output is influenced by propofol plasma concentrations, both due to *venodilation* (pooling of blood in dilated vains) [35] and myocardial depression [36].

Experimental data indicate that the transfer coefficients $a_{ij}(\cdot)$ are nonincreasing functions of the propofol concentration [35], [36]. The most widely used empirical models for pharmacodynamic concentration-effect relationships are modifications of the Hill equation [37]. Applying this almost ubiquitous empirical model to the relationship between transfer coefficients implies that

$$a_{ij}(c) = A_{ij}Q_{ij}(c), \quad Q_{ij}(c) = Q_0 \mathrm{C}_{50,ij}^{\alpha_{ij}} / \left(\mathrm{C}_{50,ij}^{\alpha_{ij}} + c^{\alpha_{ij}}\right) \tag{46}$$

where, for $i, j \in \{1,2,3\}$, $i \neq j$, $\mathrm{C}_{50,ij}$ is the drug concentration associated with a 50% decrease in the transfer coefficient, α_{ij} is a parameter that determines the steepness of the concentration-effect relationship, and A_{ij} are positive constants. Note that both pharmacokinetic parameters are functions of i and j, that is, there are distinct Hill equations for each transfer coefficient. Furthermore, since for many drugs the rate of metabolism $a_{11}(c)$ is proportional to the rate of transport of drug to the liver we assume that $a_{11}(c)$ is also proportional to the cardiac output so that $a_{11}(c) = A_{11}Q_{11}(c)$.

To illustrate the neuroadaptive control of propofol, we assume that $\mathrm{C}_{50,ij}$ and α_{ij} are independent of i and j. Also, since decreases in cardiac output are observed at clinically utilized propofol concentrations we arbitrarily assign C_{50} a value of 4 μg/ml since this value is in the midrange of clinically utilized values. We also assign α a value of 3 [38]. This value is within the typical range of those observed for ligand-receptor binding (see the discussion in [39]). The nonnegative transfer and loss coefficients A_{12}, A_{21}, A_{13}, A_{31}, and A_{11}, and the parameters $\alpha > 1$, $\mathrm{C}_{50} > 0$, and $Q_0 > 0$ are uncertain due to patient gender, weight, preexisting disease, age, and concomitant medication. Hence, the need for adaptive control to regulate intravenous anesthetics during surgery is essential.

Although propofol concentration in the blood is correlated with lack of responsiveness, and presumably consciousness [40], the concentration cannot be measured in real time during surgery. Since we are more interested in drug *effect* (depth of hypnosis) rather than drug *concentration*, we consider a model involving pharmacokinetics (drug concentration as a function of time) and pharmacodynamics (drug effect as a function of concentration) for controlling consciousness. Specifically, we use an electroencephalogram (EEG) signal as a measure of drug effect of anesthetic compounds on the brain [41]–[43]. Since electroencephalography provides real-time monitoring of the central nervous system activity, it can be used to quantify levels of consciousness, and hence, is amenable for feedback control in general anesthesia.

The BIS, an EEG indicator, has been proposed as a measure of anesthetic effect. This index quantifies the nonlinear relationships between the component frequencies in the electroencephalogram, as well as analyzing their phase and amplitude. The BIS signal is related to drug concentration by the empirical relationship

$$\mathrm{BIS}(c_{\mathrm{eff}}) = \mathrm{BIS}_0 \left(1 - \frac{c_{\mathrm{eff}}^{\gamma}}{c_{\mathrm{eff}}^{\gamma} + \mathrm{EC}_{50}^{\gamma}}\right) \tag{47}$$

where BIS_0 denotes the baseline (awake state) value and, by convention, is typically assigned a value of 100, c_{eff} is the propofol concentration in μ g/ml in the effect-site compartment (brain), EC_{50} is the concentration at half maximal effect and represents the patient's sensitivity to the drug, and γ determines the degree of nonlinearity in (47). Here, the effect-site compartment is introduced to account for finite equilibration time between the central compartment concentration and the central nervous system concentration [44].

The effect-site compartment concentration is related to the concentration in the central compartment by the first-order model [44]

$$\dot{c}_{\mathrm{eff}}(t) = a_{\mathrm{eff}}\left(c(t) - c_{\mathrm{eff}}(t)\right), \qquad c_{\mathrm{eff}}(0) = c(0); \qquad t \geq 0 \tag{48}$$

where a_{eff} in min^{-1} is a time constant. In reality, the effect-site compartment equilibrates with the central compartment in a matter of a few minutes. The parameters a_{eff}, EC_{50}, and γ are determined by data fitting and vary from patient to patient. BIS index values of 0 and 100 correspond, respectively, to an *isoelectric* EEG signal (no cerebral electrical activity) and an EEG signal of a fully conscious patient; the range between 40 and 60 indicates a moderate hypnotic state [42]. Fig. 3 shows the combined pharmacokinetic/pharmacodynamic model for the distribution of propofol.

For set-point regulation, define $e(t) \triangleq x(t) - x_{\mathrm{e}}$, where $x_{\mathrm{e}} \in \mathbb{R}_+^4$ is the set point satisfying the equilibrium condition for (43)–(45) and (48) with $x_1(t) \equiv x_{\mathrm{e}1}, x_2(t) \equiv x_{\mathrm{e}2}, x_3(t) \equiv x_{\mathrm{e}3}$, $x_4(t) = c_{\mathrm{eff}}(t) \equiv \mathrm{EC}_{50}$, and $u(t) \equiv u_{\mathrm{e}}$, so that $f_{\mathrm{e}}(e) = [f_{\mathrm{e}1}(e), f_{\mathrm{e}2}(e), f_{\mathrm{e}3}(e), f_{\mathrm{e}4}(e)]^{\mathrm{T}}$ is given by

$$\begin{aligned} f_{\mathrm{e}1}(e) = &- \left[a_{\mathrm{e}}(c) + a_{21}(c) + a_{31}(c)\right](e_1 + x_{\mathrm{e}1}) \\ &+ a_{12}(c)(e_2 + x_{\mathrm{e}2}) + a_{13}(c)(e_3 + x_{\mathrm{e}3}) \\ &- \left[a_{\mathrm{e}}(c_{\mathrm{e}}) + a_{21}(c_{\mathrm{e}}) + a_{31}(c_{\mathrm{e}})\right] x_{\mathrm{e}1} + a_{12}(c_{\mathrm{e}})x_{\mathrm{e}2} \\ &+ a_{13}(c_{\mathrm{e}})x_{\mathrm{e}3} \end{aligned} \tag{49}$$

$$\begin{aligned} f_{\mathrm{e}2}(e) = &\, a_{21}(c)(e_1 + x_{\mathrm{e}1}) - a_{12}(c)(e_2 + x_{\mathrm{e}2}) \\ &- \left[a_{21}(c_{\mathrm{e}})x_{\mathrm{e}1} - a_{12}(c_{\mathrm{e}})x_{\mathrm{e}2}\right] \end{aligned} \tag{50}$$

$$\begin{aligned} f_{\mathrm{e}3}(e) = &\, a_{31}(c)(e_1 + x_{\mathrm{e}1}) - a_{13}(c)(e_3 + x_{\mathrm{e}3}) \\ &- \left[a_{31}(c_{\mathrm{e}})x_{\mathrm{e}1} - a_{13}(c_{\mathrm{e}})x_{\mathrm{e}3}\right] \end{aligned} \tag{51}$$

$$f_{\mathrm{e}4}(e) = a_{\mathrm{eff}}\left(c - (e_4 + \mathrm{EC}_{50})\right) - a_{\mathrm{eff}}(e_{\mathrm{e}} - \mathrm{EC}_{50}) \tag{52}$$

where $c_{\mathrm{e}} \triangleq x_{\mathrm{e}1}/V_{\mathrm{c}}$. The existence of this equilibrium point follows from the fact that the Jacobian of (43)–(45) and (48) is

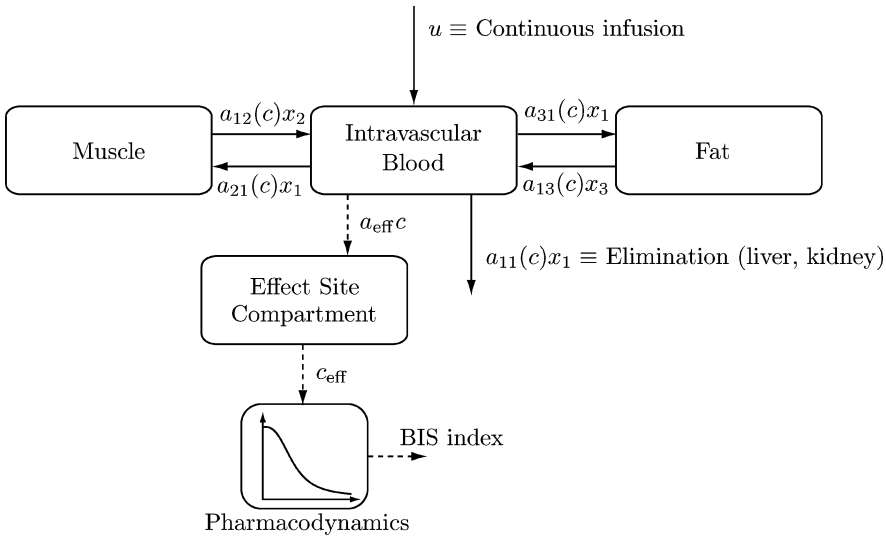

Fig. 3. Combined pharmacokinetic/pharmacodynamic model.

essentially nonnegative and every solution of (43)–(45) and (48) is bounded [6]. Next, linearizing $f_{\rm e}(e)$ about 0 and computing the eigenvalues of the resulting Jacobian matrix, it can be shown that $x_{\rm e}$ is asymptotically stable.

In the following, simulation involving the infusion of the anesthetic drug propofol, we set $\mathrm{EC}_{50} = 5.6$ μg/ml, $\gamma = 2.39$, and $\mathrm{BIS}_0 = 100$, so that the BIS signal is shown in Fig. 4. The target (desired) BIS value, $\mathrm{BIS}_{\rm target}$, is set at 50. Now, using the neuroadaptive output feedback controller

$$u(t) = \max\{0, \hat{u}(t)\} \tag{53}$$

where

$$\hat{u}(t) = -\frac{\hat{W}_1^{\rm T}(t)\sigma_1(\zeta(t))}{\hat{b} + \hat{W}_2^{\rm T}(t)\sigma_2(\zeta(t))} \tag{54}$$

$$\zeta(t) = [\mathrm{BIS}(t-d), \mathrm{BIS}(t-2d), u(t-d), u(t-2d)]^{\rm T} \tag{55}$$

$\hat{b} > 0$, $d > 0$, with update laws

$$\dot{\hat{W}}_1(t) = Q_{\mathrm{BIS}_1}\mathrm{Proj}\left[\hat{W}_1(t), -\sigma_1(\zeta(t))\,\xi_{\rm c}^{\rm T}(t)\tilde{P}B_0\right], \quad \hat{W}_1(0) = \hat{W}_{10}; \qquad t \geq 0 \tag{56}$$

$$\dot{\hat{W}}_2(t) = Q_{\mathrm{BIS}_2}\mathrm{Proj}\left[\hat{W}_2(t), -\sigma_2(\zeta(t))\,u(t)\xi_{\rm c}^{\rm T}(t)\tilde{P}B_0\right], \quad \hat{W}_2(0) = \hat{W}_{20} \tag{57}$$

where Q_{BIS_1} and Q_{BIS_2} are positive constants and $\xi_{\rm c}(t) \in \mathbb{R}^2$, $t \geq 0$, is the solution to the estimator dynamics

$$\dot{\xi}_{\rm c}(t) = A\xi_{\rm c}(t) + L\left(-\mathrm{BIS}(t) - y_{\rm c}(t) + \mathrm{BIS}_{\rm target}\right), \quad \xi_{\rm c}(0) = \xi_{\rm c0}; \qquad t \geq 0 \tag{58}$$

$$y_{\rm c}(t) = \xi_{\rm c}(t) \tag{59}$$

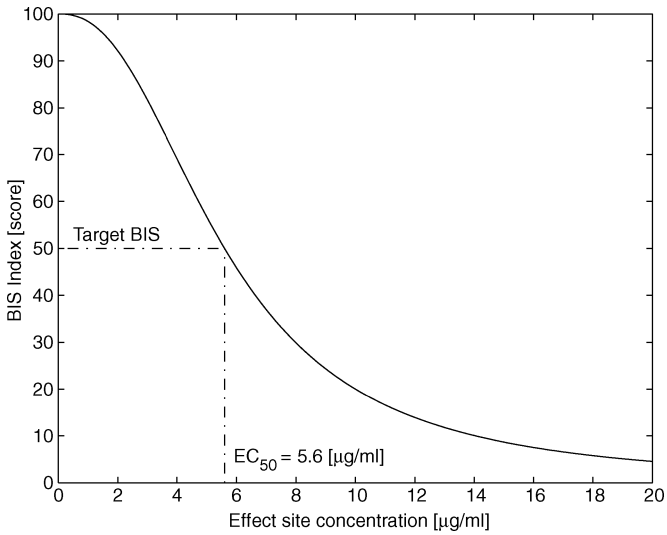

Fig. 4. BIS index versus effect site concentration.

where $A \in \mathbb{R}^{2\times 2}$ and $L \in \mathbb{R}^{2\times 1}$, it follows from Theorem 4.1 that there exist positive constants ε and T such that $|\mathrm{BIS}(t) - \mathrm{BIS}_{\rm target}| \leq \varepsilon$, $t \geq T$, for all nonnegative values of the pharmacokinetic transfer and loss coefficients A_{12}, A_{21}, A_{13}, A_{31}, and A_{11}, as well as all nonnegative coefficients α, C_{50}, and Q_0. A flowchart for the neuroadaptive control algorithm is shown in Fig. 5.

For our simulation, we assume $V_{\rm c}$ =(0.228 l/kg)(Mkg), where M = 70 kg is the mass of the patient, $A_{21}Q_0 = 0.112\,\mathrm{min}^{-1}$, $A_{12}Q_0 = 0.055\,\mathrm{min}^{-1}$, $A_{31}Q_0 = 0.0419\,\mathrm{min}^{-1}$, $A_{13}Q_0 = 0.0033$ min^{-1}, $A_{\rm e}Q_0 = 0.119$ min^{-1}, $a_{\rm eff} = 3.4657$ min^{-1}, $\alpha = 3$, and $\mathrm{C}_{50} = 4$ μg/ml [33], [38]. Note that the parameter values for α and C_{50} probably exaggerate the effect of propofol on cardiac output. They have been selected to accentuate nonlinearity but they are not biologically unrealistic. Furthermore, to illustrate the proposed neuroadaptive controller, we switch the pharmacodynamic parameters EC_{50} and γ, respectively, from 5.6 μg/ml

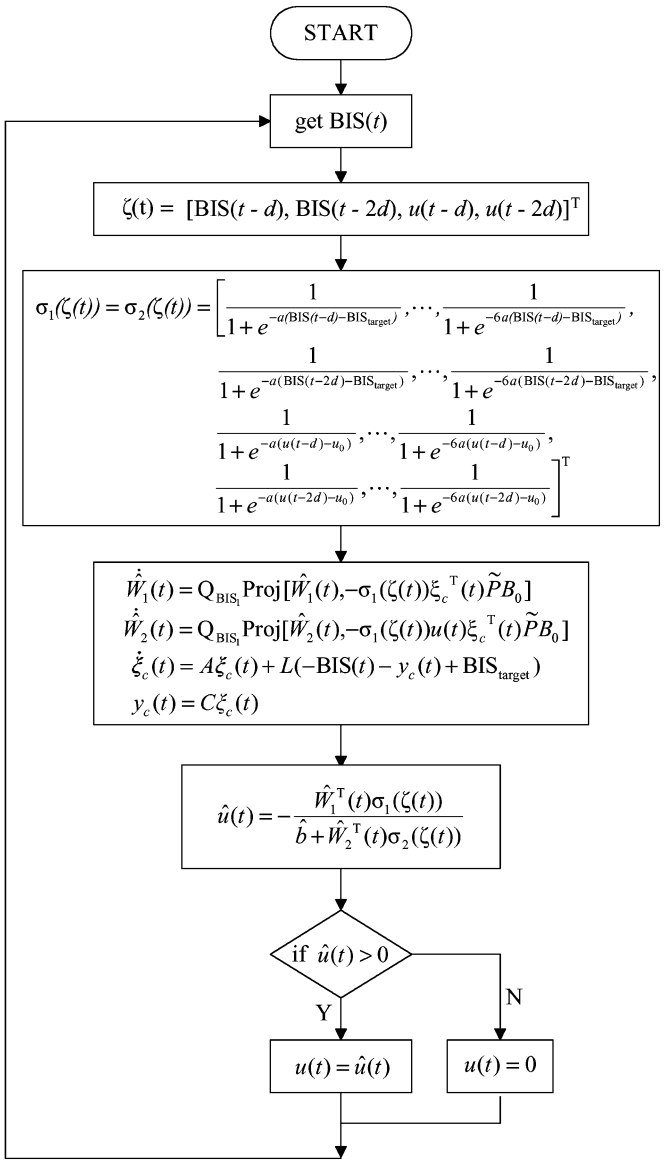

Fig. 5. Flowchart for the neuroadaptive control algorithm.

and 2.39 to 7.2 μg/ml and 3.39 at $t = 15$ min and back to 5.6μg/ml and 2.39 at $t = 30$ min. Here, we consider noncardiac surgery since cardiac surgery often utilizes hypothermia which itself changes the BIS signal. With $A = \begin{bmatrix} 0 & 1 \\ -1 & -1 \end{bmatrix}$, $L = [0,1]^{\mathrm{T}}$, $\hat{b} = 1$, $Q_{\mathrm{BIS}_1} = 2.0 \times 10^{-5}$ g/min^2, $Q_{\mathrm{BIS}_2} = 4.0 \times 10^{-5}$ g/min^2, $d = 0.005$, and initial conditions $x_1(0) = x_2(0) = x_3(0) = 0$ g, $c_{\mathrm{eff}}(0) = 0$ g/ml, $\xi_{\mathrm{c}}(0) = [0,0]^{\mathrm{T}}$, $\hat{W}_1(0) = 1 \times 10^{-3}[-3_{12\times1}, 1_{12\times1}]^{\mathrm{T}}$, and $\hat{W}_2(0) = 0_{24\times1}$, Fig. 6 shows the masses of propofol in the three compartments versus time. Fig. 7 shows the concentrations in the central and effect-site compartments versus time. Note that the effect-site compartment equilibrates with the central compartment in a matter of a few minutes. Fig. 8 shows the compensator states versus time. Finally, Fig. 9 shows the BIS index and the control signal (propofol infusion rate) versus time.

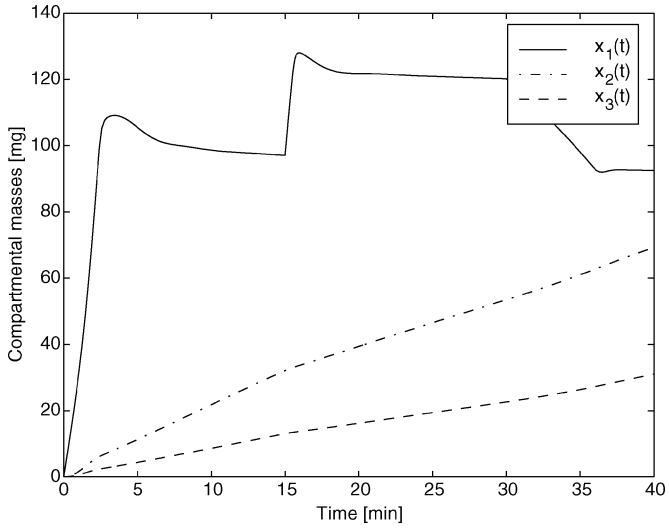

Fig. 6. Compartmental masses versus time.

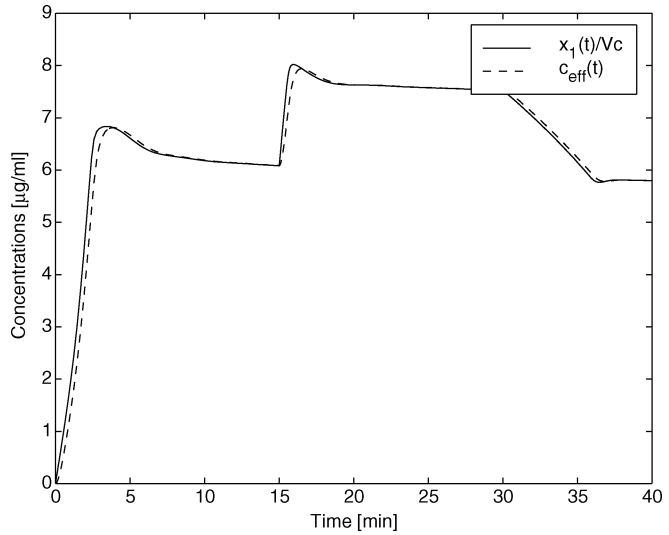

Fig. 7. Concentrations in the central and effect site compartments versus time.

For our simulation, we used

$$\begin{aligned}\sigma_1(\zeta(t)) &= \sigma_2(\zeta(t)) \\ &= \Bigg[\frac{1}{1+e^{-a(\mathrm{BIS}(t-d)-\mathrm{BIS}_{\mathrm{target}})}}, \cdots, \\ &\quad \frac{1}{1+e^{-6a(\mathrm{BIS}(t-d)-\mathrm{BIS}_{\mathrm{target}})}}, \\ &\quad \frac{1}{1+e^{-a(\mathrm{BIS}(t-2d)-\mathrm{BIS}_{\mathrm{target}})}}, \cdots, \\ &\quad \frac{1}{1+e^{-6a(\mathrm{BIS}(t-2d)-\mathrm{BIS}_{\mathrm{target}})}}, \\ &\quad \frac{1}{1+e^{-a(u(t-d)-u_0)}}, \cdots, \\ &\quad \frac{1}{1+e^{-6a(u(t-d)-u_0)}}, \\ &\quad \frac{1}{1+e^{-a(u(t-2d)-u_0)}}, \cdots, \\ &\quad \frac{1}{1+e^{-6a(u(t-2d)-u_0)}}\Bigg]^{\mathrm{T}}\end{aligned} \tag{60}$$

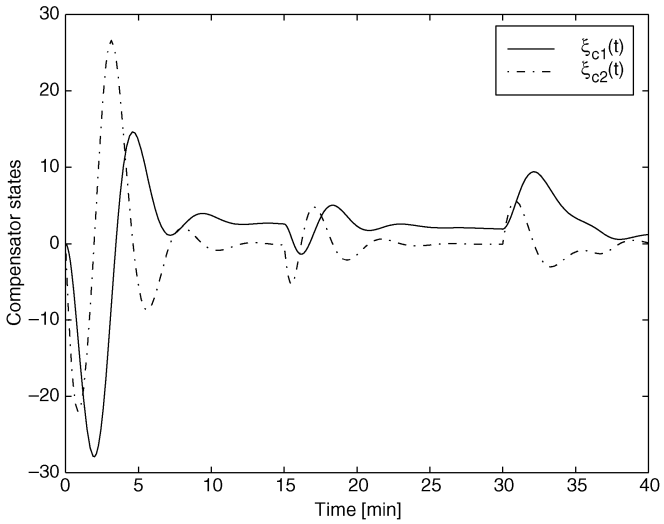

Fig. 8. Compensator states versus time.

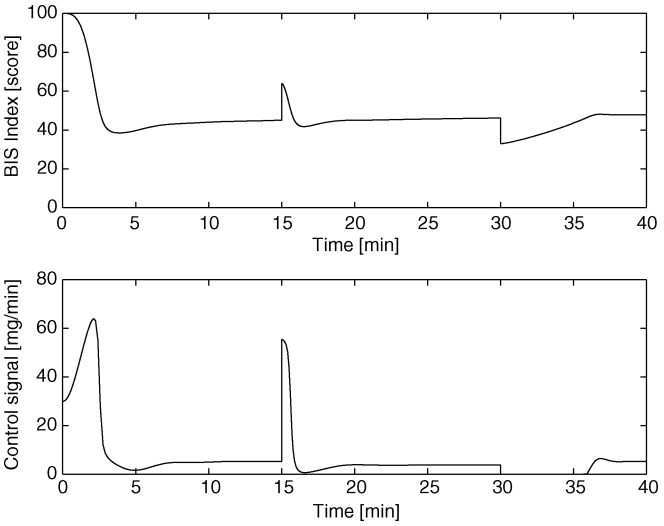

Fig. 9. BIS versus time and control signal (infusion rate) versus time.

where $s_1 = s_2 = 24$, $a = 0.1$, and $u_0 = 15$ mg/min. Even though we did not calculate the analytical bounds given by (37) due to the fact that one has to solve an optimization problem with respect to (23) and (24) to obtain ε_i^* and $w_{i\max}^*$, $i = 1, 2$, the closed-loop BIS signal response shown in Fig. 9 is clearly acceptable. Furthermore, the basis functions for $\sigma_i(\zeta)$, $i = 1, 2$, are chosen to cover the domain of interest of our pharmacokinetic/pharmacodynamic problem since we know that the BIS index varies from 0 to 100. Hence, the basis functions are distributed over that domain. The number of basis functions, however, is based on trial and error. This goes back to the Stone–Weierstrass theorem which only provides an existence result without any constructive guidelines. Finally, we note that simulations using a larger number of neurons resulted in imperceptible differences in the closed-loop system performance.

The neuroadaptive control algorithm [see (53)–(59)] does not require knowledge of the pharmacokinetic and pharmacodynamic parameters, in contrast to previous algorithms for closed-loop control of anesthesia [12], [16]. However, the neuroadaptive controller [see (53)–(59)] does not account for time delays due to the proprietary signal-averaging algorithm within the BIS monitor. The algorithm also ignores signal noise and the fact that when there is excessive noise the BIS monitor does not generate a signal, although this failure is usually brief. Only extensive clinical testing will indicate the significance of these assumptions and approximations and the direction of future algorithm development. Given the clinical observation that there is often a substantial delay between observed changes in patient status and a change in the BIS signal, other measures of depth of anesthesia may be needed [45].

VI. Clinical Evaluation Trials

We have begun clinical trials with the neuroadaptive controller shown in (53)–(59) at the Northeast Georgia Medical Center, Gainesville, GA. In initial clinical testing, we implemented (53)–(59) using a Dell Latitude C610 laptop computer with a Pentium (R) III processor running under Windows XP, an Aspect A 2000 BIS monitor (rev 3.23), and a Harvard PHD 2000 programmable research pump. The BIS monitor sends a data stream, which is updated every 5 s. This data stream contains the BIS signal as well as other parameters such as date, time, signal quality indicator, raw EEG information, and electromyographic data. The data are sent to the serial port of the laptop computer.

The infusion rate $u(t)$ for the controller is calculated by employing a forward Euler method to update the neural network weights $\hat{W}_1(t)$ and $\hat{W}_2(t)$ every 0.5 s, using the BIS signal. The infusion rate is communicated to the infusion pump using a 9600 b/min, eight data bits, two stop bits, and zero parity protocol with the aid of a USB-serial port adaptor. An updated infusion rate is sent to the pump every 1 s. Pharmacokinetic simulations predict that a pump-update every 5 s or less is adequate in the context of the algorithm under evaluation. An update interval of 1 s was selected in anticipation that future algorithms might benefit from the faster update rate.

The neuroadaptive control algorithm was programmed in Java, an object-oriented programming language chosen for its multiplatform portability tools for rapid prototyping. The program is organized into five modules, namely, bisloader, bislogger, controller, pumplogger, and pumploader. Bisloader and bislogger handle communication between the BIS monitor and the computer, while pumploader and pumplogger manage the Harvard pump apparatus. The module bisloader finds the serial port that receives the BIS signal by using the Java class CommPort identifier, and then invokes bislogger. Bislogger uses the Java class SerialPort EventListener to read the signal, and uses the class StringTokenizer to parse the BIS signal from the input stream. The infusion rate is calculated by the controller module. Finally, pumploader opens the serial port communicating to the pump and establishes the communication protocol, while pumplogger delivers the infusion rate to the pump.

The protocol for clinical evaluation of the system was approved by the Institutional Review Board of Northeast Georgia Medical Center. Patients are enrolled after giving informed consent. Our protocol excludes patients requiring emergency

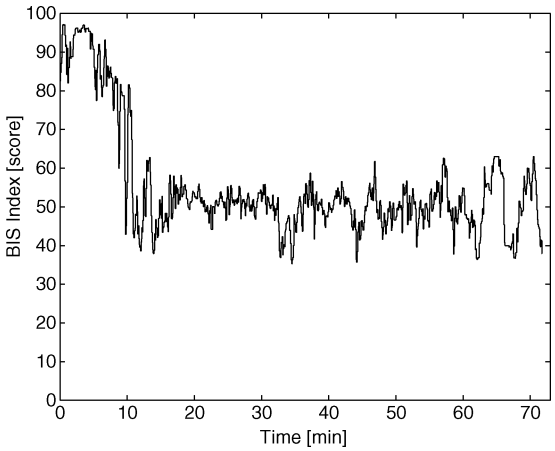

Fig. 10. Controlled BIS index versus time for the neuroadaptive controller.

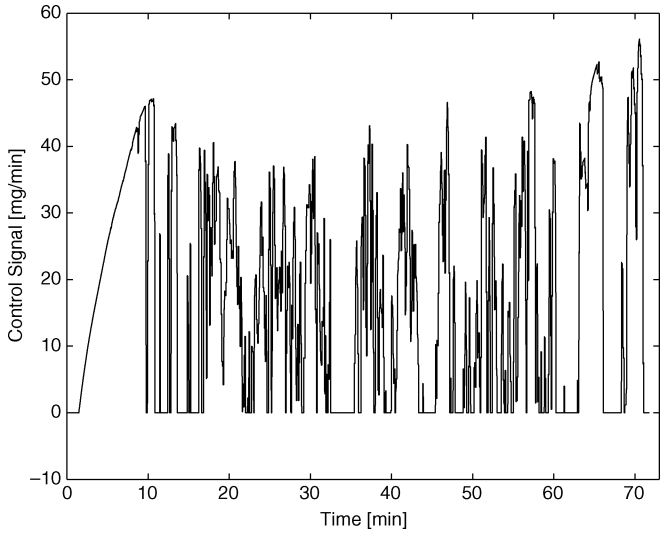

Fig. 11. Infusion rate versus time for the neuroadaptive controller.

surgery, pediatric patients, hemodynamically unstable patients, and patients for whom we anticipate difficult airway management. Otherwise, all elective surgical patients who can provide informed consent are candidates. Preoperative management, including administration of antianxiolytic drugs, is left to the discretion of the attending anesthesiologist. Propofol is delivered using the BIS-computer-pump system with a target value of 50. In addition to propofol, all patients receive infusions of either sufentanil or fentanyl with loading doses of 2 or 0.25 μg/ml and continuous infusions of 2 or 0.25 (μg/ml)/h, respectively, to provide analgesia. To ensure patient safety, an independent anesthesia provider observes the progress of the study and can terminate the study if it appears that the patient's safety is being jeopardized by either overdosing or underdosing of propofol.

To date, we have performed seven clinical trials with the neuroadaptive contoller. For the last clinical trial, Figs. 10 and 11 show the controlled BIS index and the control signal versus time of the adaptive and neuroadaptive controller, respectively. These results are typical of all seven clinical trials. In all our design studies, no initial propofol dose is administered by the anesthesiologist. Induction of anesthesia is delivered by the neuroadaptive controller. In some of the clinical trials, we have observed a slight overshoot at the induction of anesthesia with the BIS signal dropping below the target. We suspect that the initial target overshoot stems from the signal averaging time delays within the BIS monitor. In addition, the BIS signal and propofol infusion rate oscillations are due to measurement noise in the BIS signal.

VII. Conclusion

Nonnegative and compartmental dynamical systems are widely used to capture system dynamics involving the interchange of mass and energy between homogenous subsystems or compartments. Thus, it is not surprising that nonnegative and compartmental models are remarkably effective in describing the dynamical behavior of biological, physiological, and pharmacological systems. In this paper, we developed a neural adaptive dynamic output feedback control framework for adaptive set-point regulation of nonlinear uncertain nonnegative and compartmental systems. Using Lyapunov methods, the proposed framework was shown to guarantee ultimate boundedness of the error signals corresponding to the physical system states and the neural network weighting gains, while additionally guaranteeing the nonnegativity of the closed-loop system states associated with the plant dynamics.

A nonlinear four-compartment pharmacokinetic and pharmacodynamic patient model for the disposition of anesthetic drug propofol was developed, and the proposed neuroadaptive control framework was used to monitor and control a desired constant level of consciousness for noncardiac surgery. In addition, we validated our neuroadaptive feedback control algorithm via a series of clinical evaluation trials. The clinical trials demonstrated excellent regulation of unconsciousness allowing for a safe and effective administration of the anesthetic agent propofol. Even though measurement noise was not addressed in our framework, it should be noted that EEG signals may have as much as 10% variation due to noise. In particular, the BIS signal may be corrupted by *electromyographic noise*, that is, signals emanating from muscle rather than the central nervous system. Although electromyographic noise can be minimized by muscle paralysis, there are other sources of measurement noise, such as electrocautery and x-ray, that need to be accounted for within the control design process. This is evident in Figs. 10 and 11. Future work will involve extensions to adaptive output feedback controllers with measurement noise and disturbance rejection guarantees.

While our objective in this paper was to develop a control design methodology for ICU sedation and intraoperative anesthesia, the results of this paper can have implications for other uses of closed-loop control of drug delivery. There are numerous potential applications such as control of glucose, heart rate, blood pressure, etc. Finally, we note that the range of applications of the proposed controller design framework is not limited to biological and medical systems. Specifically, epidemiology, ecology, economic systems, telecommunications systems, transportation systems, and power systems, to cite but a few examples, all lead to nonnegative dynamical systems.

APPENDIX

To prove Theorem 4.1, first, define

$$\hat{W}_{1u}(t) \triangleq \begin{cases} \hat{W}_1(t), & \text{if } \hat{u}(t) \geq\geq 0 \\ 0, & \text{otherwise} \end{cases}. \tag{61}$$

Next, defining $e_\xi(t) \triangleq \xi(t) - \xi_\mathrm{e}$, $e_z(t) \triangleq z(t) - z_\mathrm{e}$, and $\tilde{\xi}(t) \triangleq \xi_\mathrm{c}(t) - e_\xi(t)$, and using (15)–(21), (23), (24), and (30), it follows from (15), (16), and (35):

$$\begin{aligned}
\dot{e}_\xi(t) &= Ae_\xi(t) + A\xi_\mathrm{e} + \tilde{f}_\mathrm{u}\left(\xi(t), z(t)\right) + G_\xi\left(\xi(t), z(t)\right) u(t) \\
&= Ae_\xi(t) + B_0 \\
&\quad \times \left[f_\mathrm{u}\left(\mathcal{T}\left(x(t)\right)\right) - f_\mathrm{u}\left(\mathcal{T}(x_\mathrm{e})\right) - \hat{G}\left(\mathcal{T}(x_\mathrm{e})\right) u_\mathrm{e} \right] \\
&\quad + B_0 \hat{G}\left(\mathcal{T}\left(x(t)\right)\right) u(t) \\
&\quad + B_0 \left(\hat{B} + \hat{W}_2^\mathrm{T}(t) \left[I_m \otimes \sigma_2\left(\zeta(t)\right) \right] \right) \\
&\quad \times \left(-u(t) - \left(\hat{B} + \hat{W}_2^\mathrm{T}(t) \left[I_m \otimes \sigma_2\left(\zeta(t)\right) \right] \right)^{-1} \right. \\
&\qquad \left. \times \hat{W}_{1u}^\mathrm{T}(t) \sigma_1\left(\zeta(t)\right) \right) \\
&= Ae_\xi(t) + B_0 \left[W_1^\mathrm{T} \hat{\sigma}_1\left(x(t)\right) + \varepsilon_1\left(x(t)\right) \right] \\
&\quad + B_0 \left(W_2^\mathrm{T} \left[I_m \otimes \hat{\sigma}_2\left(x(t)\right) \right] + \varepsilon_2\left(x(t)\right) \right) u(t) \\
&\quad - B_0 \hat{W}_2^\mathrm{T}(t) \left[I_m \otimes \sigma_2\left(\zeta(t)\right) \right] u(t) \\
&\quad - B_0 \hat{W}_{1u}^\mathrm{T}(t) \sigma_1\left(\zeta(t)\right) \\
&= Ae_\xi(t) + B_0 \left[W_1^\mathrm{T} \hat{\sigma}_1\left(x(t)\right) - W_1^\mathrm{T} \sigma_1\left(\zeta(t)\right) \right. \\
&\qquad \left. + W_1^\mathrm{T} \sigma_1\left(\zeta(t)\right) + \varepsilon_1\left(x(t)\right) \right] \\
&\quad + B_0 \left(W_2^\mathrm{T} \left[I_m \otimes \hat{\sigma}_2\left(x(t)\right) \right] - W_2^\mathrm{T} \left[I_m \otimes \sigma_2\left(\zeta(t)\right) \right] \right. \\
&\qquad \left. + W_2^\mathrm{T} \left[I_m \otimes \sigma_2\left(\zeta(t)\right) \right] + \varepsilon_2\left(x(t)\right) \right) u(t) \\
&\quad - B_0 \hat{W}_2^\mathrm{T}(t) \left[I_m \otimes \sigma_2\left(\zeta(t)\right) \right] u(t) \\
&\quad - B_0 \hat{W}_{1u}^\mathrm{T}(t) \sigma_1\left(\zeta(t)\right) \\
&= Ae_\xi(t) - B_0 \tilde{W}_1^\mathrm{T}(t) \sigma_1\left(\zeta(t)\right) \\
&\quad - B_0 \tilde{W}_2^\mathrm{T}(t) \left[I_m \otimes \sigma_2\left(\zeta(t)\right) \right] u(t) \\
&\quad + B_0 \left(\hat{W}_1(t) - \hat{W}_{1u}(t) \right)^\mathrm{T} \sigma_1\left(\zeta(t)\right) + B_0 \varepsilon_1\left(x(t)\right) \\
&\quad + B_0 \varepsilon_2\left(x(t)\right) u(t) + B_0 W_1^\mathrm{T} \left[\hat{\sigma}_1\left(x(t)\right) - \sigma_1\left(\zeta(t)\right) \right] \\
&\quad + B_0 W_2^\mathrm{T} \left[I_m \otimes \left(\hat{\sigma}_2\left(x(t)\right) - \sigma_2\left(\zeta(t)\right) \right) \right] u(t), \\
&\quad e_\xi(0) = \xi_0 - \xi_\mathrm{e}; \qquad t \geq 0,
\end{aligned} \tag{62}$$

$$\dot{e}_z(t) = \tilde{f}_z\left(e_\xi(t), e_z(t)\right), \qquad e_z(0) = z_0 - z_\mathrm{e} \tag{63}$$

and

$$\begin{aligned}
\dot{\tilde{\xi}}(t) &= \dot{\xi}_\mathrm{c}(t) - \dot{e}_\xi(t) \\
&= \tilde{A}\tilde{\xi}(t) + B_0 \tilde{W}_1^\mathrm{T}(t) \sigma_1\left(\zeta(t)\right) \\
&\quad + B_0 \tilde{W}_2^\mathrm{T}(t) \left[I_m \otimes \sigma_2\left(\zeta(t)\right) \right] u(t) \\
&\quad - B_0 \left(\hat{W}_1(t) - \hat{W}_{1u}(t) \right)^\mathrm{T} \sigma_1\left(\zeta(t)\right) - B_0 \varepsilon_1\left(x(t)\right) \\
&\quad + B_0 \varepsilon_2\left(x(t)\right) u(t) - B_0 W_1^\mathrm{T} \left[\hat{\sigma}_1\left(x(t)\right) - \sigma_1\left(\zeta(t)\right) \right] \\
&\quad - B_0 W_2^\mathrm{T} \left[I_m \otimes \left(\hat{\sigma}_2\left(x(t)\right) - \sigma_2\left(\zeta(t)\right) \right) \right] u(t), \\
&\quad \tilde{\xi}(0) = \xi_{c0} - \xi_0 + \xi_\mathrm{e}
\end{aligned} \tag{64}$$

where $\tilde{A} \triangleq A - LC$, $\tilde{f}_z(e_\xi, e_z) \triangleq f_z(e_\xi + x_\mathrm{e}, e_z + z_\mathrm{e})$, $\tilde{W}_i(t) \triangleq \hat{W}_i(t) - W_i$, $i = 1, 2$, and $\hat{\sigma}_1 : \mathbb{R}^n \to \mathbb{R}^{s_1}$ and $\hat{\sigma}_2 : \mathbb{R}^n \to \mathbb{R}^{s_2}$ are such that each component of $\hat{\sigma}_1(\cdot)$ and $\hat{\sigma}_2(\cdot)$ takes values between 0 and 1.

To show ultimate boundedness of the closed-loop system (32), (33), and (62)–(64), consider the Lyapunov-like function

$$\begin{aligned}
V(e_\xi, e_z, \tilde{\xi}, \tilde{W}_1, \tilde{W}_2) &= e_\xi^\mathrm{T} P e_\xi + \tilde{\xi}^\mathrm{T} \tilde{P} \tilde{\xi} \\
&\quad + \mathrm{tr} \tilde{W}_1 Q_1^{-1} \tilde{W}_1^\mathrm{T} + \mathrm{tr} \tilde{W}_2 Q_2^{-1} \tilde{W}_2^\mathrm{T}
\end{aligned} \tag{65}$$

where $P > 10$ and $\tilde{P} > 0$ satisfy (34) and (41), respectively. Note that (65) satisfies (4) with $x_1 = [e_\xi^\mathrm{T}, \tilde{\xi}^\mathrm{T}, (\mathrm{vec}\, \hat{W}_1)^\mathrm{T}, (\mathrm{vec}\, \hat{W}_2)^\mathrm{T}]^\mathrm{T}$, $x_2 = e_z$, and $\alpha(\|x_1\|) = \beta(\|x_1\|) = \|x_1\|^2$, where $\|x_1\|^2 \triangleq e_\xi^\mathrm{T} P e_\xi + \tilde{\xi}^\mathrm{T} \tilde{P} \tilde{\xi} + \mathrm{tr}\, \tilde{W}_1 Q_1^{-1} \tilde{W}_1^\mathrm{T} + \mathrm{tr}\, \tilde{W}_2 Q_2^{-1} \tilde{W}_2^\mathrm{T}$ and $\mathrm{vec}(\cdot)$ denotes the column stacking operator. Furthermore, $\alpha(\|x_1\|)$ is a class $\mathcal{K}_\infty$ function. Now, letting $e_\xi(t)$ and $\xi_\mathrm{c}(t)$, $t \geq 0$, denote the solution to (62) and (35), respectively, and using (23), (24), (27), (32), and (33), it follows that the time derivative of $V(e_\xi, e_z, \tilde{\xi}, \tilde{W}_1, \tilde{W}_2)$ along the closed-loop system trajectories is given by

$$\begin{aligned}
&\dot{V}\left(e_\xi(t), e_z(t), \tilde{\xi}(t), \tilde{W}_1(t), \tilde{W}_2(t)\right) \\
&\quad = 2e_\xi^\mathrm{T}(t) P \left[Ae_\xi(t) - B_0 \tilde{W}_1^\mathrm{T}(t) \sigma_1\left(\zeta(t)\right) - B_0 \tilde{W}_2^\mathrm{T}(t) \right. \\
&\qquad \times \left[I_m \otimes \sigma_2\left(\zeta(t)\right) \right] u(t) + B_0 \\
&\qquad \times \left(\hat{W}_1(t) - \hat{W}_{1u}(t) \right)^\mathrm{T} \sigma_1\left(\zeta(t)\right) + B_0 \varepsilon_1\left(x(t)\right) \\
&\qquad + B_0 \varepsilon_2\left(x(t)\right) u(t) + B_0 W_1^\mathrm{T} \\
&\qquad \times \left[\hat{\sigma}_1\left(x(t)\right) - \sigma_1\left(\zeta(t)\right) \right] + B_0 W_2^\mathrm{T} \\
&\qquad \left. \times \left[I_m \otimes \left(\hat{\sigma}_2\left(x(t)\right) - \sigma_2\left(\zeta(t)\right) \right) \right] u(t) \right] \\
&\quad + 2\tilde{\xi}^\mathrm{T}(t) \tilde{P} \left[\tilde{A}\tilde{\xi}(t) + B_0 \tilde{W}_1^\mathrm{T}(t) \sigma_1\left(\zeta(t)\right) + B_0 \tilde{W}_2^\mathrm{T}(t) \right. \\
&\qquad \times \left[I_m \otimes \sigma_2\left(\zeta(t)\right) \right] u(t) - B_0 \\
&\qquad \times \left(\hat{W}_1(t) - \hat{W}_{1u}(t) \right)^\mathrm{T} \sigma_1\left(\zeta(t)\right) \\
&\qquad - B_0 \varepsilon_1\left(x(t)\right) + B_0 \varepsilon_2\left(x(t)\right) u(t) - B_0 W_1^\mathrm{T} \\
&\qquad \times \left[\hat{\sigma}_1\left(x(t)\right) - \sigma_1\left(\zeta(t)\right) \right] - B_0 W_2^\mathrm{T} \\
&\qquad \left. \times \left[I_m \otimes \left(\hat{\sigma}_2\left(x(t)\right) - \sigma_2\left(\zeta(t)\right) \right) \right] u(t) \right] \\
&\quad + 2\mathrm{tr} \tilde{W}_1^\mathrm{T}(t) Q_1^{-1} \dot{\hat{W}}_1(t) + 2\mathrm{tr} \tilde{W}_2^\mathrm{T}(t) Q_2^{-1} \dot{\hat{W}}_2(t) \\
&\quad = -e_\xi^\mathrm{T}(t) R e_\xi(t) - \tilde{\xi}^\mathrm{T}(t) \tilde{R} \tilde{\xi}(t) - 2e_\xi^\mathrm{T}(t) P B_0 \tilde{W}_1^\mathrm{T}(t) \\
&\qquad \times \sigma_1\left(\zeta(t)\right) - 2e_\xi^\mathrm{T}(t) P B_0 \tilde{W}_2^\mathrm{T}(t) \left[I_m \otimes \sigma_2\left(\zeta(t)\right) \right] u(t) \\
&\qquad + 2e_\xi^\mathrm{T}(t) P B_0 \left(\hat{W}_1(t) - \hat{W}_{1u}(t) \right)^\mathrm{T} \sigma_1\left(\zeta(t)\right) + 2e_\xi^\mathrm{T}(t) \\
&\qquad \times P B_0 \left(\varepsilon_1\left(x(t)\right) + \varepsilon_2\left(x(t)\right) u(t) \right) + 2e_\xi^\mathrm{T}(t) P B_0 \\
&\qquad \times \left(W_1^\mathrm{T} \left[\hat{\sigma}_1\left(x(t)\right) - \sigma_1\left(\zeta(t)\right) \right] + W_2^\mathrm{T} \right. \\
&\qquad \left. \times \left[I_m \otimes \left(\hat{\sigma}_2\left(x(t)\right) - \sigma_2\left(\zeta(t)\right) \right) \right] u(t) \right) \\
&\qquad + 2\tilde{\xi}^\mathrm{T}(t) \tilde{P} B_0 \tilde{W}_1^\mathrm{T}(t) \sigma_1\left(\zeta(t)\right) + 2\tilde{\xi}^\mathrm{T}(t) \tilde{P} B_0 \tilde{W}_2^\mathrm{T}(t) \\
&\qquad \times \left[I_m \otimes \sigma_2\left(\zeta(t)\right) \right] u(t) - 2\tilde{\xi}^\mathrm{T}(t) \tilde{P} B_0 \\
&\qquad \times \left(\hat{W}_1(t) - \hat{W}_{1u}(t) \right)^\mathrm{T} \sigma_1\left(\zeta(t)\right) - 2\tilde{\xi}^\mathrm{T}(t) \tilde{P} B_0 \\
&\qquad \times \left(\varepsilon_1\left(x(t)\right) + \varepsilon_2\left(x(t)\right) u(t) \right) - 2\tilde{\xi}^\mathrm{T}(t) \tilde{P} B_0 \\
&\qquad \times \left(W_1^\mathrm{T} \left[\hat{\sigma}_1\left(x(t)\right) - \sigma_1\left(\zeta(t)\right) \right] \right. \\
&\qquad \left. + W_2^\mathrm{T} \left[I_m \otimes \left(\hat{\sigma}_2\left(x(t)\right) - \sigma_2\left(\zeta(t)\right) \right) \right] u(t) \right) \\
&\qquad + 2\mathrm{tr} \tilde{W}_1^\mathrm{T}(t) \mathrm{Proj}\left(\hat{W}_1(t), -\sigma_1\left(\zeta(t)\right) \xi_\mathrm{c}^\mathrm{T}(t) \tilde{P} B_0 \right) \\
&\qquad + 2\mathrm{tr} \tilde{W}_2^\mathrm{T}(t)
\end{aligned}$$

$$
\begin{aligned}
&\times \operatorname{Proj}\left(\hat{W}_2(t), -\left[I_m \otimes \sigma_2\left(\zeta(t)\right)\right] u(t) \xi_{\mathrm{c}}^{\mathrm{T}}(t) \tilde{P} B_0\right) \\
&\leq -\lambda_{\min}(RP^{-1}) \left\| P^{1/2} e_\xi(t) \right\|^2 \\
&\quad - \lambda_{\min}(\tilde{R}\tilde{P}^{-1}) \left\| \tilde{P}^{1/2} \tilde{\xi}(t) \right\|^2 \\
&\quad - 2 e_\xi^{\mathrm{T}}(t)(P+\tilde{P}) B_0 \tilde{W}_1^{\mathrm{T}}(t) \sigma_1\left(\zeta(t)\right) - 2 e_\xi^{\mathrm{T}}(t) \\
&\quad \times (P+\tilde{P}) B_0 \tilde{W}_2^{\mathrm{T}}(t) \left[I_m \otimes \sigma_2\left(\zeta(t)\right)\right] u(t) \\
&\quad + 2 e_\xi^{\mathrm{T}}(t) P B_0 \left(\varepsilon_1\left(x(t)\right) + \varepsilon_2\left(x(t)\right) u(t)\right) + 2 e_\xi^{\mathrm{T}}(t) \\
&\quad \times P B_0 \left(W_1^{\mathrm{T}} \left[\hat{\sigma}_1\left(x(t)\right) - \sigma_1\left(\zeta(t)\right)\right]\right. \\
&\qquad \left. + W_2^{\mathrm{T}} \left[I_m \otimes \left(\hat{\sigma}_2\left(x(t)\right) - \sigma_2\left(\zeta(t)\right)\right)\right] u(t)\right) \\
&\quad - 2 \tilde{\xi}^{\mathrm{T}}(t) \tilde{P} B_0 \left(\varepsilon_1\left(x(t)\right) + \varepsilon_2\left(x(t)\right) u(t)\right) - 2 \tilde{\xi}^{\mathrm{T}}(t) \\
&\quad \times \tilde{P} B_0 \left(W_1^{\mathrm{T}} \left[\hat{\sigma}_1\left(x(t)\right) - \sigma_1\left(\zeta(t)\right)\right]\right. \\
&\qquad \left. + W_2^{\mathrm{T}} \left[I_m \otimes \left(\hat{\sigma}_2\left(x(t)\right) - \sigma_2\left(\zeta(t)\right)\right)\right] u(t)\right) \\
&\quad + 2 \left(e_\xi^{\mathrm{T}}(t) P - \tilde{\xi}^{\mathrm{T}}(t) \tilde{P}\right) B_0 \left(\hat{W}_1(t) - \hat{W}_{1u}(t)\right)^{\mathrm{T}} \\
&\quad \times \sigma_1\left(\zeta(t)\right) + 2 \operatorname{tr} \tilde{W}_1^{\mathrm{T}}(t) \\
&\quad \times \left[\operatorname{Proj}\left(\hat{W}_1(t), -\sigma_1\left(\zeta(t)\right) \xi_{\mathrm{c}}^{\mathrm{T}}(t) \tilde{P} B_0\right)\right. \\
&\qquad \left. + \sigma_1\left(\zeta(t)\right) \xi_{\mathrm{c}}^{\mathrm{T}}(t) \tilde{P} B_0\right] + 2 \operatorname{tr} \tilde{W}_2^{\mathrm{T}}(t) \\
&\quad \times \left[\operatorname{Proj}\left(\hat{W}_2(t), -\left[I_m \otimes \sigma_2\left(\zeta(t)\right)\right] u(t) \xi_{\mathrm{c}}^{\mathrm{T}}(t) \tilde{P} B_0\right)\right. \\
&\qquad \left. + \left[I_m \otimes \sigma_2\left(\zeta(t)\right)\right] u(t) \xi_{\mathrm{c}}^{\mathrm{T}}(t) \tilde{P} B_0\right] \\
&\leq -\lambda_{\min}(RP^{-1}) \left\| P^{1/2} e_\xi(t) \right\|^2 \\
&\quad - \lambda_{\min}(\tilde{R}\tilde{P}^{-1}) \left\| \tilde{P}^{1/2} \tilde{\xi}(t) \right\|^2 - 2 e_\xi^{\mathrm{T}}(t)(P+\tilde{P}) \\
&\quad \times B_0 \tilde{W}_1^{\mathrm{T}}(t) \sigma_1\left(\zeta(t)\right) - 2 e_\xi^{\mathrm{T}}(t)(P+\tilde{P}) B_0 \tilde{W}_2^{\mathrm{T}}(t) \\
&\quad \times \left[I_m \otimes \sigma_2\left(\zeta(t)\right)\right] u(t) + 2 e_\xi^{\mathrm{T}}(t) P B_0 \\
&\quad \times \left(\varepsilon_1\left(x(t)\right) + \varepsilon_2\left(x(t)\right) u(t)\right) + 2 e_\xi^{\mathrm{T}}(t) P B_0 \\
&\quad \times \left(W_1^{\mathrm{T}} \left[\hat{\sigma}_1\left(x(t)\right) - \sigma_1\left(\zeta(t)\right)\right]\right. \\
&\qquad \left. + W_2^{\mathrm{T}} \left[I_m \otimes \left(\hat{\sigma}_2\left(x(t)\right) - \sigma_2\left(\zeta(t)\right)\right)\right] u(t)\right) \\
&\quad - 2 \tilde{\xi}^{\mathrm{T}}(t) \tilde{P} B_0 \left(\varepsilon_1\left(x(t)\right) + \varepsilon_2\left(x(t)\right) u(t)\right) - 2 \tilde{\xi}^{\mathrm{T}}(t) \tilde{P} B_0 \\
&\quad \times \left(W_1^{\mathrm{T}} \left[\hat{\sigma}_1\left(x(t)\right) - \sigma_1\left(\zeta(t)\right)\right]\right. \\
&\qquad \left. + W_2^{\mathrm{T}} \left[I_m \otimes \left(\hat{\sigma}_2\left(x(t)\right) - \sigma_2\left(\zeta(t)\right)\right)\right] u(t)\right) \\
&\quad + 2 \left(e_\xi^{\mathrm{T}}(t) P - \tilde{\xi}^{\mathrm{T}}(t) \tilde{P}\right) B_0 \left(\hat{W}_1(t) - \hat{W}_{1u}(t)\right)^{\mathrm{T}} \\
&\quad \times \sigma_1\left(\zeta(t)\right). \qquad (66)
\end{aligned}
$$

For the two cases given in (61), the last term on the right-hand side of (66) gives the following.

1) If $\hat{u}(t) \geq\geq 0$, then $\hat{W}_{1u}(t) = \hat{W}_1(t)$, and hence

$$
2 \left(e_\xi^{\mathrm{T}}(t) P - \tilde{\xi}^{\mathrm{T}}(t) \tilde{P}\right) B_0 \left(\hat{W}_1(t) - \hat{W}_{1u}(t)\right)^{\mathrm{T}} \sigma_1\left(\zeta(t)\right) = 0.
$$

2) Otherwise, $\hat{W}_{1u}(t) = 0$, and hence

$$
\begin{aligned}
&2 \left(e_\xi^{\mathrm{T}}(t) P - \tilde{\xi}^{\mathrm{T}}(t) \tilde{P}\right) B_0 \left(\hat{W}_1(t) - \hat{W}_{1u}(t)\right)^{\mathrm{T}} \sigma_1\left(\zeta(t)\right) \\
&\quad = 2 \left(e_\xi^{\mathrm{T}}(t) P - \tilde{\xi}^{\mathrm{T}}(t) \tilde{P}\right) B_0 \hat{W}_1^{\mathrm{T}}(t) \sigma_1\left(\zeta(t)\right) \\
&\quad \leq 2 \sqrt{s_1} \hat{w}_{1\max} \| P^{1/2} B_0 \| \left\| P^{1/2} e_\xi(t) \right\| \\
&\qquad + 2 \sqrt{s_1} \hat{w}_{1\max} \| \tilde{P}^{1/2} B_0 \| \left\| \tilde{P}^{1/2} \tilde{\xi}(t) \right\|.
\end{aligned}
$$

Hence, it follows from (66) that in either case:

$$
\begin{aligned}
&\dot{V}\left(e_\xi(t), e_z(t), \tilde{\xi}(t), \tilde{W}_1(t), \tilde{W}_2(t)\right) \\
&\quad \leq -\lambda_{\min}(RP^{-1}) \left\| P^{1/2} e_\xi(t) \right\|^2 \\
&\qquad - \lambda_{\min}(\tilde{R}\tilde{P}^{-1}) \left\| \tilde{P}^{1/2} \tilde{\xi}(t) \right\|^2 \\
&\qquad + 2 \sqrt{s_1} \hat{w}_{1\max} \left\| P^{-1/2} (P + \tilde{P}) B_0 \right\| \left\| P^{1/2} e_\xi(t) \right\| \\
&\qquad + 2 \sqrt{m s_2} \hat{w}_{2\max} u^* \left\| P^{-1/2} (P + \tilde{P}) B_0 \right\| \left\| P^{1/2} e_\xi(t) \right\| \\
&\qquad + 2 \left(\varepsilon_1^* + \varepsilon_2^* u^*\right) \| P^{1/2} B_0 \| \left\| P^{1/2} e_\xi(t) \right\| \\
&\qquad + 2 (\sqrt{s_1} \hat{w}_{1\max} + \sqrt{m s_2} \hat{w}_{2\max} u^*) \| P^{1/2} B_0 \| \\
&\qquad \times \left\| P^{1/2} e_\xi(t) \right\| + 2 (\sqrt{s_1} \hat{w}_{1\max} + \sqrt{m s_2} \hat{w}_{2\max} u^*) \\
&\qquad \times \| \tilde{P}^{1/2} B_0 \| \left\| \tilde{P}^{1/2} \tilde{\xi}(t) \right\| \\
&\qquad + 2 \left(\varepsilon_1^* + \varepsilon_2^* u^*\right) \| \tilde{P}^{1/2} B_0 \| \left\| \tilde{P}^{1/2} \tilde{\xi}(t) \right\| \\
&\qquad + 2 \sqrt{s_1} \hat{w}_{1\max} \| P^{1/2} B_0 \| \left\| P^{1/2} e_\xi(t) \right\| \\
&\qquad + 2 \sqrt{s_1} \hat{w}_{1\max} \| \tilde{P}^{1/2} B_0 \| \left\| \tilde{P}^{1/2} \tilde{\xi}(t) \right\| \\
&\quad = -\lambda_{\min}(RP^{-1}) \left(\left\| P^{1/2} e_\xi(t) \right\| - \alpha_1 \right)^2 \\
&\qquad - \lambda_{\min}(\tilde{R}\tilde{P}^{-1}) \left(\left\| \tilde{P}^{1/2} \tilde{\xi}(t) \right\| - \alpha_2 \right)^2 + \nu \qquad (67)
\end{aligned}
$$

where ν, α_1, and α_2 are given by (38) and (40), respectively. Now, for

$$
\| P^{1/2} e_\xi \| \geq \sqrt{\frac{\nu}{\lambda_{\min}(RP^{-1})}} + \alpha_1 \qquad (68)
$$

or

$$
\| \tilde{P}^{1/2} \tilde{\xi} \| \geq \sqrt{\frac{\nu}{\lambda_{\min}(\tilde{R}\tilde{P}^{-1})}} + \alpha_2 \qquad (69)
$$

it follows that $\dot{V}(e_\xi(t), e_z(t), \tilde{\xi}(t), \tilde{W}_1(t), \tilde{W}_2(t)) \leq 0$ for all $t \geq 0$, that is, $\dot{V}(e_\xi(t), e_z(t), \tilde{\xi}(t), \tilde{W}_1(t), \tilde{W}_2(t)) \leq 0$ for all $(e_\xi(t), e_z(t), \tilde{\xi}(t), \tilde{W}_1(t), \tilde{W}_2(t)) \in \tilde{\mathcal{D}}_{\mathrm{e}} \setminus \tilde{\mathcal{D}}_{\mathrm{r}}$ and $t \geq 0$, where (see Fig. 12)

$$
\begin{aligned}
\tilde{\mathcal{D}}_{\mathrm{e}} \triangleq \Big\{ &(e_\xi, e_z, \tilde{\xi}, \tilde{W}_1, \tilde{W}_2) \in \mathbb{R}^m \times \mathbb{R}^{n-m} \\
&\times \mathbb{R}^r \times \mathbb{R}^{s_1 \times m} \times \mathbb{R}^{m s_2 \times m} : x \in \mathcal{D}_{\mathrm{c}} \Big\} \qquad (70)
\end{aligned}
$$

$$
\begin{aligned}
\tilde{\mathcal{D}}_{\mathrm{r}} \triangleq \Big\{ &(e_\xi, e_z, \tilde{\xi}, \tilde{W}_1, \tilde{W}_2) \in \mathbb{R}^m \times \mathbb{R}^{n-m} \times \mathbb{R}^r \times \mathbb{R}^{s_1 \times m} \\
&\times \mathbb{R}^{m s_2 \times m} : \| P^{1/2} e_\xi \| \leq \alpha_{e_\xi}, \| \tilde{P}^{1/2} \tilde{\xi} \| \leq \alpha_{\tilde{\xi}} \Big\}. \qquad (71)
\end{aligned}
$$

Next, define

$$
\begin{aligned}
\tilde{\mathcal{D}}_\alpha \triangleq \Big\{ &(e_\xi, e_z, \tilde{\xi}, \tilde{W}_1, \tilde{W}_2) \in \mathbb{R}^m \times \mathbb{R}^{n-m} \times \mathbb{R}^r \times \mathbb{R}^{s_1 \times m} \\
&\times \mathbb{R}^{m s_2 \times m} : V(e_\xi, e_z, \tilde{\xi}, \tilde{W}_1, \tilde{W}_2) \leq \alpha \Big\} \qquad (72)
\end{aligned}
$$

where α is the maximum value such that $\tilde{\mathcal{D}}_\alpha \subseteq \tilde{\mathcal{D}}_{\mathrm{e}}$, and define

$$
\begin{aligned}
\tilde{\mathcal{D}}_\eta \triangleq \Big\{ &(e_\xi, e_z, \tilde{\xi}, \tilde{W}_1, \tilde{W}_2) \in \mathbb{R}^m \times \mathbb{R}^{n-m} \times \mathbb{R}^r \times \mathbb{R}^{s_1 \times m} \\
&\times \mathbb{R}^{m s_2 \times m} : V(e_\xi, e_z, \tilde{\xi}, \tilde{W}_1, \tilde{W}_2) \leq \eta \Big\} \qquad (73)
\end{aligned}
$$

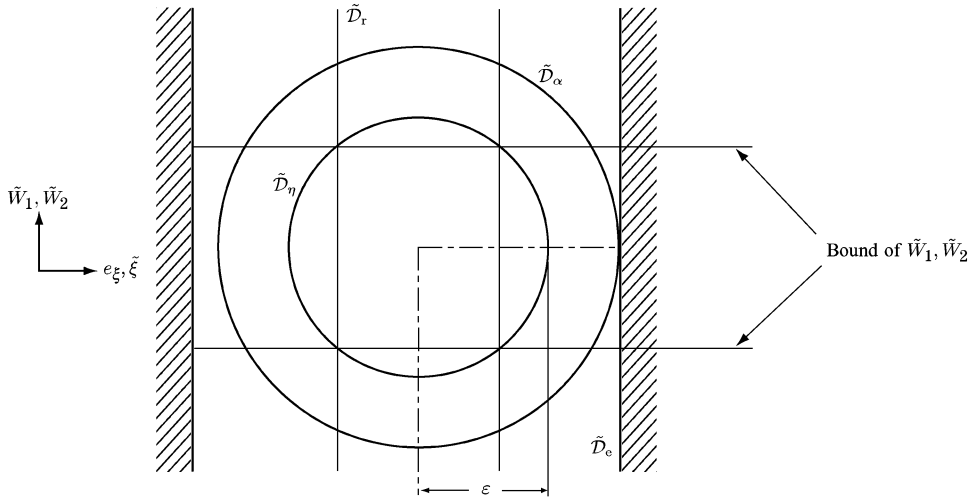

Fig. 12. Visualization of sets used in the proof of Theorem 4.1.

where

$$\begin{aligned}\eta > \beta(\mu) &= \mu \\ &= \alpha_{e_\xi}^2 + \alpha_{\tilde{\xi}}^2 + \lambda_{\max}\left(Q_1^{-1}\right)\hat{w}_{1\max}^2 \\ &\quad + \lambda_{\max}\left(Q_2^{-1}\right)\hat{w}_{2\max}^2. \end{aligned} \tag{74}$$

To show ultimate boundedness of the closed-loop system (32), (33), and (62)–(64) assume[2] that $\tilde{\mathcal{D}}_{\eta} \subset \tilde{\mathcal{D}}_{\alpha}$ (see Fig. 12). Now, since $\dot{V}(e_\xi, e_z, \tilde{\xi}, \tilde{W}_1, \tilde{W}_2) \leq 0$ for all $(e_\xi, e_z, \tilde{\xi}, \tilde{W}_1, \tilde{W}_2) \in \tilde{\mathcal{D}}_{\mathrm{e}} \setminus \tilde{\mathcal{D}}_{\mathrm{r}}$ and $\tilde{\mathcal{D}}_{\mathrm{r}} \subset \tilde{\mathcal{D}}_{\alpha}$, it follows that $\tilde{\mathcal{D}}_{\alpha}$ is positively invariant. Hence, if $(e_\xi(0), e_z(0), \tilde{\xi}(0), \tilde{W}_1(0), \tilde{W}_2(0)) \in \tilde{\mathcal{D}}_{\alpha}$, then it follows from Theorem 3.2 that the solution $(e_\xi(t), e_z(t), \tilde{\xi}(t), \hat{W}(t)), t \geq 0$, to (32), (33), and (62)–(64) are ultimately bounded with respect to $(e_\xi, \tilde{\xi}, \tilde{W}_1, \tilde{W}_2)$ uniformly in $e_z(0)$ with ultimate bound given by $\varepsilon = \alpha^{-1}(\eta) = \sqrt{\eta}$ which yields (37). In addition, since (63) is input-to-state stable with e_ξ viewed as the input, it follows from Proposition 3.1 that the solution $e_z(t)$, $t \geq 0$, to (63) is also ultimately bounded.

Next, it follows from [46, Th. 1] that there exist a continuously differentiable, radially unbounded, positive–definite function $V_z : \mathbb{R}^{n_z} \to \mathbb{R}$ and class $\mathcal{K}$ functions $\gamma_1(\cdot)$ and $\gamma_2(\cdot)$ such that

$$V_z'(e_z)\tilde{f}_z(e_\xi, e_z) \leq -\gamma_1\left(\|e_z\|\right), \qquad \|e_z\| \geq \gamma_2\left(\|e_\xi\|\right). \tag{75}$$

Since the upper bound for $\|e_\xi\|^2$ is given by η, it follows that the set given by:

$$\mathcal{D}_z \triangleq \left\{ z \in \mathbb{R}^{n-r} : V_z(z - z_{\mathrm{e}}) \leq \max_{\|z - z_{\mathrm{e}}\| = \gamma_2(\sqrt{\eta})} V_z(z - z_{\mathrm{e}}) \right\} \tag{76}$$

is also positively invariant. Now, since $\tilde{\mathcal{D}}_{\alpha}$ and $\mathcal{D}_z$ are positively invariant, it follows:

$$\begin{aligned}\mathcal{D}_\alpha \triangleq \Big\{ &(x, \tilde{\xi}, \tilde{W}_1, \tilde{W}_2) \in \mathbb{R}^n \times \mathbb{R}^r \times \mathbb{R}^{s_1 \times m} \times \mathbb{R}^{m s_2 \times m} : \\ &V(\xi - y_{\mathrm{d}}, z - e_z, \tilde{\xi}, \hat{W}_1 - W_1, \hat{W}_2 - W_2) \leq \alpha \Big\} \end{aligned} \tag{77}$$

[2]This assumption is standard in the neural network literature and ensures that, in the error space $\mathcal{D}_{\mathrm{e}}$, there exists at least one Lyapunov level set $\mathcal{D}_\eta \subset \mathcal{D}_\alpha$. In the case where the neural network approximation holds in $\mathbb{R}^n$ with delayed values, this assumption is automatically satisfied. See the discussion at the end of Theorem 4.1 for further details.

is also positively invariant. In addition, since (32), (33), and (62)–(64) are ultimately bounded with respect to $(e_\xi, \tilde{\xi}, \tilde{W}_1, \tilde{W}_2)$ and (63) is input-to-state stable with e_ξ viewed as the input, it follows from Proposition 3.1 that the solution $(e_\xi(t), e_z(t), \tilde{\xi}(t), \tilde{W}_1(t), \tilde{W}_2(t))$, $t \geq 0$, of the closed-loop system (32), (33) and (62)–(64) is ultimately bounded for all $(e_\xi(0), e_z(0), \tilde{\xi}(0), \tilde{W}_1(0), \tilde{W}_2(0)) \in \tilde{\mathcal{D}}_{\alpha}$.

Finally, $u(t) \geq\geq 0$, $t \geq 0$, is a restatement of (30). Now, since $G(x(t)) \geq\geq 0$, $t \geq 0$, and $u(t) \geq\geq 0$, $t \geq 0$, it follows from Proposition 2.1 that $x(t) \geq\geq 0$, $t \geq 0$, for all $x_0 \in \overline{\mathbb{R}}_+^n$. □

REFERENCES

[1] P. G. Welling, *Pharmacokinetics: Processes, Mathematics, and Applications*, 2nd ed. Washington, DC: Amer. Chemical Soc., 1997.

[2] J. A. Jacquez, *Compartmental Analysis in Biology and Medicine*. Ann Arbor, MI: Univ. Michigan Press, 1985.

[3] W. Sandberg, "On the mathematical foundations of compartmental analysis in biology, medicine and ecology," *IEEE Trans. Circuits Syst.*, vol. CS-25, no. 5, pp. 273–279, May 1978.

[4] D. H. Anderson, *Compartmental Modeling and Tracer Kinetics*. Berlin, Germany: Springer-Verlag, 1983.

[5] K. Godfrey, *Compartmental Models and Their Applications*. New York: Academic, 1983.

[6] J. A. Jacquez and C. P. Simon, "Qualitative theory of compartmental systems," *SIAM Rev.*, vol. 35, pp. 43–79, 1993.

[7] W. M. Haddad and V. Chellaboina, "Stability and dissipativity theory for nonnegative dynamical systems: A unified analysis framework for biological and physiological systems," *Nonlinear Anal.: Real World Appl.*, vol. 6, pp. 35–65, 2005.

[8] J. M. Bailey and W. M. Haddad, "Drug-dosing control in clinical pharmacology: Paradigms, benefits, and challenges," *Control Syst. Mag.*, vol. 25, pp. 35–51, 2005.

[9] W. G. He, H. Kaufman, and R. J. Roy, "Multiple model adaptive control procedures for blood pressure control," *IEEE Trans. Biomed. Eng.*, vol. BME-33, no. 1, pp. 10–19, Jan. 1986.

[10] R. R. Rao, B. Aufderheide, and B. W. Bequette, "Experimental studies on multiple-model predictive control for automated regulation of hemodynamic variables," *IEEE Trans. Biomed. Eng.*, vol. 50, no. 3, pp. 277–288, Mar. 2003.

[11] R. G. Bickford, "Automatic electroencephalographic control of anesthesia (servoanesthesia)," *Electroencephalographic Clin. Neurophysiol.*, vol. 3, pp. 83–86, 1951.

[12] H. Schwilden, J. Schutler, and H. Stoeckel, "Closed-loop feedback control of methohexital anesthesia by quantitative EEG analysis in humans," *Anesthesiology*, vol. 67, pp. 341–347, 1987.

[13] P. S. Glass, M. Bloom, L. Kearse, C. Rosow, P. Sebel, and P. Manberg, "Bispectral analysis measures sedation and memory effects of propofol, midazolam, isoflurane, and alfentanil in normal volunteers," *Anesthesiology*, vol. 86, pp. 836–847, 1997.

[14] P. S. Sebel, E. Lang, I. J. Rampil, P. F. White, R. Cork, M. Jopling, N. T. Smith, P. S. Glass, and P. Manberg, "A multicenter study of bispectral electroencephalogram analysis for monitoring anesthetic effect," *Anesthesia Analgesia*, vol. 84, pp. 891–899, 1997.
[15] A. R. Absalom, N. Sutcliffe, and G. N. Kenny, "Closed-loop control of anesthesia using bispectral index. Performance assessment in patients undergoing major orthopedic surgery under combined general and regional anesthesia," *Anesthesiology*, vol. 96, pp. 67–73, 2002.
[16] M. M. R. F. Struys, T. D. Smet, L. F. M. Versichelen, R. V. den Broecke, and E. P. Mortier, "Comparison of closed-loop controlled administration of propofol using BIS as the controlled variable versus "standard practice" controlled administration," *Anesthesiology*, vol. 95, pp. 6–17, 2001.
[17] P. S. A. Glass and I. J. Rampil, "Automated anesthesia: Fact or fantasy," *Anesthesiology*, vol. 95, pp. 1–2, 2001.
[18] F. L. Lewis, S. Jagannathan, and A. Yesildirak, *Neural Network Control of Robot Manipulators and Nonlinear Systems*. London, U.K.: Taylor & Francis, 1999.
[19] N. Hovakimyan, F. Nardi, A. Calise, and N. Kim, "Adaptive output feedback control of uncertain nonlinear systems using single-hidden-layer neural networks," *IEEE Trans. Neural Netw.*, vol. 13, no. 6, pp. 1420–1431, Nov. 2002.
[20] N. Hovakimyan, B.-J. Yang, and A. J. Calise, "Adaptive output feedback control methodology applicable for non-minimum phase systems," *Automatica*, vol. 42, pp. 513–522, 2006.
[21] T. Hayakawa, W. M. Haddad, J. M. Bailey, and N. Hovakimyan, "Passivity-based neural network adaptive output feedback control for nonlinear nonnegative dynamical systems," *IEEE Trans. Neural Netw.*, vol. 16, no. 2, pp. 387–398, Mar. 2005.
[22] A. Berman, M. Neumann, and R. J. Stern, *Nonnegative Matrices in Dynamic Systems*. New York: Wiley, 1989.
[23] A. Berman and R. J. Plemmons, *Nonnegative Matrices in the Mathematical Sciences*. New York: Academic, 1979.
[24] D. S. Bernstein and D. C. Hyland, "Compartmental modeling and second-moment analysis of state space systems," *SIAM J. Matrix Anal. Appl.*, vol. 14, pp. 880–901, 1993.
[25] D. S. Bernstein and S. P. Bhat, "Nonnegativity, reducibility, and semistability of mass action kinetics," in *Proc. IEEE Conf. Decision Control*, Phoenix, AZ, Dec. 1999, pp. 2206–2211.
[26] H. K. Khalil, *Nonlinear Systems*. Upper Saddle River, NJ: Prentice-Hall, 1996.
[27] H. L. Royden, *Real Analysis*. New York: Macmillan, 1988.
[28] C. I. Byrnes and A. Isidori, "Asymptotic stabilization of minimum phase nonlinear systems," *IEEE Trans. Autom. Control*, vol. 36, no. 10, pp. 1122–1137, Oct. 1991.
[29] A. Isidori, *Nonlinear Control Systems*. New York: Springer-Verlag, 1995.
[30] C.-T. Chen, *Linear System Theory and Design*. New York: Holt, Rinehart and Winston, 1984.
[31] E. Lavretsky, N. Hovakimyan, and A. J. Calise, "Upper bounds for approximation of continuous-time dynamics using delayed outputs and feedforward neural networks," *IEEE Trans. Autom. Control*, vol. 48, no. 9, pp. 1606–1610, Sep. 2003.
[32] P. De Leenheer and D. Aeyels, "Stabilization of positive linear systems," *Syst. Control Lett.*, vol. 44, pp. 259–271, 2001.
[33] B. Marsh, M. White, N. Morton, and G. N. Kenny, "Pharmacokinetic model driven infusion of propofol in children," *Brit. J. Anaesth.*, vol. 67, pp. 41–48, 1991.
[34] R. N. Upton, G. I. Ludrook, C. Grant, and A. Martinez, "Cardiac output is a determinant of the initial concentration of propofol after short-term administration," *Anethesia Analgesia*, vol. 89, pp. 545–552, 1999.
[35] M. Muzi, R. A. Berens, J. P. Kampine, and T. J. Ebert, "Venodilation contributes to propofol-mediated hypotension in humans," *Anethesia Analgesia*, vol. 74, pp. 877–883, 1992.
[36] E. F. Ismail, S. J. Kim, and M. R. Salem, "Direct effects of propofol on myocardial contractility in situ canine hearts," *Anesthesiology*, vol. 79, pp. 964–972, 1992.
[37] A. V. Hill, "The possible effects of the aggregation of the molecules of haemoglobin on its dissociation curves," *J. Physiol.*, vol. 40, pp. iv–vii, 1910.
[38] T. Kazama, K. Ikeda, K. Morita, M. Kikura, M. Doi, T. Ikeda, and T. Kurita, "Comparison of the effect site Ke0s of propofol for blood pressure and EEG bispectral index in elderly and young patients," *Anesthesiology*, vol. 90, pp. 1517–1527, 1999.
[39] R. G. Eckenhoff and J. S. Johansson, "On the relevance of "clinically relevant concentrations" of inhaled anesthetics in in vitro experiments," *Anesthesiology*, vol. 91, pp. 856–860, 1999.
[40] T. Kazama, K. Ikeda, and K. Morita, "The pharmacodynamic interaction between propofol and fentanyl with respect to the suppression of somatic or hemodynamic responses to skin incision, peritoneum incision, and abdominal wall retraction," *Anesthesiology*, vol. 89, pp. 894–906, 1998.
[41] P. S. Glass, M. Bloom, L. Kearse, C. Rosow, P. Sebel, and P. Manberg, "Bispectral analysis measures sedation and memory effects of propofol, midazolam, isoflurane, and alfentanil in normal volunteers," *Anesthesiology*, vol. 86, pp. 836–847, 1997.
[42] J. C. Sigl and N. G. Chamoun, "An introduction to bispectral analysis for the electroencephalogram," *J. Clin. Monit.*, vol. 10, pp. 392–404, 1994.
[43] E. Mortier, M. Struys, T. De Smet, L. Versichelen, and G. Rolly, "Closed-loop controlled administration of propofol using bispectral analysis," *Anaesthesia*, vol. 53, pp. 749–754, 1998.
[44] T. W. Schnider, C. F. Minto, and D. R. Stanski, "The effect compartment concept in pharmacodynamic modelling," *Anaes. Pharmacol. Rev.*, vol. 2, pp. 204–213, 1994.
[45] X. S. Zhang, R. J. Roy, and E. W. Jensen, "EEG complexity as a measure of depth of anesthesia for patients," *IEEE Trans. Biomed. Eng.*, vol. 48, no. 12, pp. 1424–1433, Dec. 2001.
[46] E. D. Sontag and Y. Wang, "On characterizations of the input-to-state stability property," *Syst. Control Lett.*, vol. 24, pp. 351–359, 1995.

Wassim M. Haddad (S'87–M'87–SM'01) received the B.S., M.S., and Ph.D. degrees in mechanical engineering from the Florida Institute of Technology, Melbourne, in 1983, 1984, and 1987, respectively, with specialization in dynamical systems and control.

From 1987 to 1994, he served as a consultant for the Structural Controls Group of the Government Aerospace Systems Division, Harris Corporation, Melbourne, FL. In 1988, he joined the faculty of the Mechanical and Aerospace Engineering Department at Florida Institute of Technology where he founded and developed the Systems and Control Option within the graduate program. Since 1994, he has been a member of the faculty in the School of Aerospace Engineering at Georgia Institute of Technology where he holds the rank of a Professor. His research contributions in linear and nonlinear dynamical systems and control are documented in over 450 archival journal and conference publications. He is the coauthor of the books *Hierarchical Nonlinear Switching Control Design with Applications to Propulsion Systems* (New York: Springer-Verlag, 2000), *Thermodynamics: A Dynamical Systems Approach* (Princeton, NJ: Princeton Univ. Press, 2005), *Impulsive and Hybrid Dynamical Systems: Stability, Dissipativity, and Control* (Princeton, NJ: Princeton Univ. Press, 2006), and *Nonlinear Dynamical Systems and Control: A Lyapunaov-Based Approach* (Princeton, NJ: Princeton Univ. Press, 2007, to appear). His recent research is concentrated on nonlinear robust and adaptive control, nonlinear dynamical system theory, large-scale systems, hierarchical nonlinear switching control, analysis and control of nonlinear impulsive and hybrid systems, system thermodynamics, thermodynamic modeling of mechanical and aerospace systems, network systems, nonlinear analysis and control for biological and physiological systems, and active control for clinical pharmacology.

Dr. Haddad is a National Science Foundation Presidential Faculty Fellow and a member of the Academy of Nonlinear Sciences.

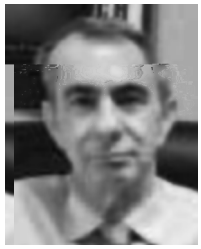

James M. Bailey received the B.S. degree in premedical studies from the Davidson College, Charlotte, NC, in 1969, the Ph.D. degree in chemistry (physical) from the University of North Carolina, Chapel Hill, in 1973, and the M.D. degree from the Southern Illinois University School of Medicine, Springfield, in 1982.

He was a Helen Hay Whitney Fellow at the California Institute of Technology, Pasadena, from 1973 to 1975 and an Assistant Professor of chemistry and biochemistry at the Southern Illinois University from 1975 to 1979. After receiving the M.D. degree, he completed the residency in anesthesiology and then a fellowship in cardiac anesthesiology at the Emory University School of Medicine affiliated hospitals. From 1986 to 2002, he was an Assistant Professor of anesthesiology and then Associate Professor of anesthesiology at Emory, where he also served as the Director of the critical care service. In September 2002, he moved his clinical practice to Northeast Georgia

Medical Center, Gainesville, as the Director of cardiac anesthesia and Consultant in critical care medicine. He remains affiliated with the Emory University School of Medicine Department of Anesthesiology as a Clinical Associate Professor. He is board-certified in anesthesiology, critical care medicine, and transesophageal echocardiography. He is the author or coauthor of 98 journal articles, conference publications, or book chapters. His research interests have focused on pharmacokinetic and pharmacodynamic modeling of anesthetic and vasoactive drugs and, more recently, applications of dynamical system theory in medicine.

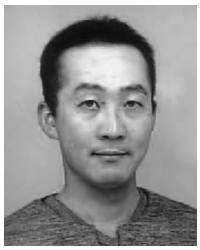

Tomohisa Hayakawa (S'00–M'04) received the B.Eng. degree in aeronautical engineering from the Kyoto University, Kyoto, Japan, in 1997, the M.S. degree in aerospace engineering from the State University of New York (SUNY), Buffalo, NY, in 1999, and the M.S. degree in applied mathematics and the Ph.D. degree in aerospace engineering both from Georgia Institute of Technology, Atlanta, in 2001 and 2003, respectively.

After serving as a Research Fellow at the Department of Aeronautics and Astronautics, Kyoto University, and at the Japan Science and Technology Agency (JST), he joined the Department of Mechanical and Environmental Informatics, Tokyo Institute of Technology, Tokyo, Japan, in 2006, where he is an Associate Professor. His research interests include stability of nonlinear systems, nonnegative and compartmental systems, hybrid systems, nonlinear adaptive control, neural networks and intelligent control, stochastic dynamical systems, and applications to aerospace vehicles, multiagent systems, robotic systems, financial dynamics, and biological/biomedical systems.

Naira Hovakimyan (M'01–SM'02) received the Ph.D. degree in physics and mathematics from the Institute of Applied Mathematics of Russian Academy of Sciences, Moscow, Russia, in 1992.

She joined the Institute of Mechanics at the Armenian Academy of Sciences as a Research Scientist, where she worked until 1997. In 1997, she was awarded a governmental postdoctoral scholarship to work in INRIA, France. The subject areas in which she has published include differential pursuit-evasion games, optimal control of robotic manipulators, robust control, and adaptive estimation and control. In 1998, she was invited to the School of Aerospace Engineering of Georgia Technology University, Atlanta, where she worked as a Research Faculty Member until 2003. In 2003, she joined the Department of Aerospace and Ocean Engineering, Virginia Polytechnic Institute and State University, Blacksburg, as an Associate Professor. She is the author of over 100 refereed publications. Her current interests are in the theory of adaptive control and estimation, neural networks, and stability theory.

Dr. Hovakimyan is the Associate Fellow of the American Institute of Aeronautics and Astronautics (AIAA), the member of the American Mathematical Society (AMS) and the International Society of Dynamic Games (ISDG), and she is serving as an Associate Editor for the IEEE Control Systems Society, IEEE TRANSACTIONS ON NEURAL NETWORKS, IEEE TRANSACTIONS ON CONTROL SYSTEMS TECHNOLOGY, *Computational Management Science of Springer*, *International Journal of Control*, and *Systems and Automation*. She is the 2004 and 2005 recipient of Pride@Boeing award. She is the recipient of the Society of Instrument and Control Engineers (SICE) International scholarship for the best paper of a Young Investigator at the VII ISDG Symposium (Japan, 1996).